THE TECTONIC EXPRESSION SLAB PULL AT CONTINENTAL CONVERGENT BOUNDARIES

Leigh H. Royden
Department of Earth, Atmospheric, and Planetary Sciences,
Massachusetts Institute of Technology, Cambridge

Abstract. Examination of five thrust belt systems developed at continental subduction boundaries suggests that they comprise two distinct groups that display pronounced and systematic differences in structural style, topographic elevation, denudation, metamorphism, postcollisional convergence, and foredeep basin geometry and facies. The distinctive geological features developed within each thrust belt group appear to be causally linked to the relative rates of subduction and convergence via the magnitude of horizontal compressional stress transmitted across the subduction boundary. At subduction boundaries where the rate of overall plate convergence is less than the rate of subduction (termed here retreating subduction boundaries) the transmission of horizontal compressive stress across the plate boundary is small, and regional deformation of the overriding plate is by horizontal extension. The tectonic expression of these retreating subduction boundaries includes topographically low mountains, little erosion or denudation, low-grade to no metamorphism, little to no involvement of crystalline basement in shortening, little to no postcollisional convergence, anomalously deep foredeep basins, and a protracted history of flysch deposition within the adjacent foredeep basin. Analysis of deflection and gravity data across three retreating subduction boundaries (Apennine, Carpathian and Hellenic systems) shows that subduction is driven by gravitational forces acting on dense subducted slabs at depths between about 40 and 80 km (Carpathians), 50 and 150 km (Apennines) and 50 and 250 km (Hellenides). The total mass anomalies represented by the slabs are approximately 3×10^{12} , 6×10^{12} and 12×10^{12} N/m, respectively. The slabs are partially supported by flexural stresses transmitted through the subducted lithosphere to the foreland, and partially supported by dynamic (viscous) stresses in the asthenosphere. At subduction boundaries where the rate of overall plate convergence is greater than the rate of subduction (termed here advancing subduction boundaries) the transmission of horizontal compressive stress across the plate boundary is large, and regional deformation of the overriding plate is by horizontal shortening. The tectonic expression of these advancing subduction boundaries includes topographically high mountains, antithetic thrust belts, large amounts of erosion and denudation, exposure of high-grade metamorphic rocks at the surface, extensive deformation of crystalline basement to midcrustal depths, protracted postcollisional convergence (tens of millions of years), and a protracted history of molasse deposition within the adjacent foredeep basins. Analysis of gravity and deflection data across two advancing subduction boundaries developed within the continental lithosphere (Western to Eastern and Southern Alps and Himalayas) shows

Copyright 1993 by the American Geophysical Union.

that the thrust sheets have been translated for great distances over the foreland lithosphere (relative to the point at which the subduction forces are applied), thus obscuring any flexural and gravity signals from the subducted slab. However, it appears that far-field stresses, presumably related to global plate motions, drive most of the convergent motion across these subduction boundaries. The concept that orogenic belts formed above retreating subduction boundaries have recognizable tectonic signatures that differ from those of orogenic belts formed above advancing subduction boundaries suggests that it may be possible to interpret the plate boundary settings in which ancient orogenic belts evolved.

INTRODUCTION

Many authors have noted that wherever plate convergence rates are exceeded by subduction rates at oceanic subduction boundaries, upper plate extension (usually in a back arc or interarc position) occurs within the overriding plate. Subsequent attempts to interpret this phenomenon in terms of stress transmission across oceanic subduction systems and the forces that drive subduction have been partially successful. For example, Molnar and Atwater [1978] showed that back arc extensional basins are more likely to form at subduction boundaries where the subducted plate has a high density (old oceanic lithosphere) and across which the rate of large-scale plate convergence is low, while other authors have observed that the largest intermediate-depth earthquakes occur only within subduction systems that lack active back arc extension [Uyeda and Kanamori, 1979; Ruff and Kanamori, 1980]. Such studies indicate a relationship between the density of the downgoing lithosphere, the rate of subduction, the rate of large-scale plate convergence, and the transmission of horizontal compressive stresses between the overriding and downgoing plates [e.g. Cross and Pilger, 1982; Jarrard, 1986a,b].

More recently, it has been proposed that at continental subduction boundaries the relative rates of subduction and plate convergence can be correlated not only with the presence or absence of regional upper plate extension but also with the structure and morphology of the associated orogenic belts [Royden and Burchfiel, 1989]. In their analysis, thrust belts formed at subduction boundaries within the continental lithosphere can be divided into two distinct classes depending on the relative rates of subduction and large-scale plate convergence (as evidenced by the presence or absence of regional upper plate extension), and these two classes of orogenic belts exhibit pronounced and systematic differences in topographic elevation, structural expression, metamorphism, and foreland basin development. Perhaps of greatest interest is the insight that these orogenic systems can provide about the forces that drive subduction of the downgoing plates and the way in which these forces are consistently expressed through surface deformation. In this paper, these large-scale plate boundary processes and the consequent surface deformation are examined through examples from a variety of active and recently active orogenic belts.

SUBDUCTION RATE VERSUS CONVERGENCE RATE: GEOMETRICAL IMPLICATIONS

The rate of overall plate convergence can be defined as the rate of convergence between points located in the rigid, interior

portions of the upper and lower plates and outside of the zone of plate boundary deformation, which in the continents may be up to 1000 km or more in width (points A and B in Figure 1). In this paper the rate of subduction is defined as the rate of convergence between a point in the rigid interior of the downgoing plate and the outer part of the trench or foreland basin located in front of the subduction zone (points A and C in Figure 1). In this framework the rate of change in length of line AB corresponds to the rate of overall plate convergence, while the rate of change in length of line AC corresponds to the rate of subduction (sometimes called the rate of trench roll-back).

Subduction boundaries can be roughly grouped into plate boundaries across which the rate of convergence exceeds the rate of subduction, and plate boundaries across which the rate of subduction exceeds the rate of convergence. Where the rate of convergence exceeds the rate of subduction, horizontal shortening must occur in the overriding plate (roughly equal to the change in length of line BC). In extreme cases, much of the overall convergence may be taken up by upper plate shortening (for example, Pliocene-Quaternary convergence across the Himalayas and Tibet; Molnar and Deng [1984] and Lyon-Caen and Molnar [1985]). This type of plate boundary will be referred to as an advancing subduction boundary because the trench or foreland basin is advancing toward the rigid interior part of the overriding plate as evidenced by shortening of the overriding plate (e.g., along line BC).

Where the rate of subduction exceeds the rate of convergence, horizontal extension must occur in the overriding plate. In extreme cases, there may be no net plate convergence, and the rate of subduction is balanced by an equal rate of extension within the overriding plate (for example, the Carpathian-Pannonian Basin in middle Miocene time; Royden 1988a). This type of plate boundary will be referred to as a

retreating subduction boundary, because the trench or foreland basin is retreating from the rigid interior part of the overriding plate as evidenced by extension of the overriding plate (e.g. along line BC). Within continental lithosphere, upper plate extension can occur in a back arc, interarc or forearc position (see examples discussed below). Although thrust belts and local horizontal shortening also occur within these extensional systems, the regional deformation mode is extensional, and shortening occurs only within a narrow belt at the leading edge of the overriding plate, where sedimentary rocks are scraped from the downgoing plate and accreted onto the base of the overriding plate in the continental equivalent of an accretionary prism.

THE GEOLOGICAL EXPRESSION OF THRUST BELTS FORMED AT ADVANCING AND RETREATING SUBDUCTION BOUNDARIES

Retreating subduction boundaries are distinguished from advancing subduction boundaries by a wide variety of geological features. Examples taken from five orogenic systems serve to illustrate the systematic geological differences between the two classes of subduction boundary (Figures 2 and 3). Of these five orogenic systems, two have developed above advancing subduction zones (the Western to Eastern Alps and the Himalayas) while the remaining three have developed above retreating subduction zones, as evidenced by significant back arc extension contemporaneous with subduction (the Apennines, the Carpathians and the Hellenides). These particular belts were selected because they are active or recently active and because their geological history, structural and timing relations, and tectonic setting are well known. Gravity profiles are available across each of the thrust belts and the associated

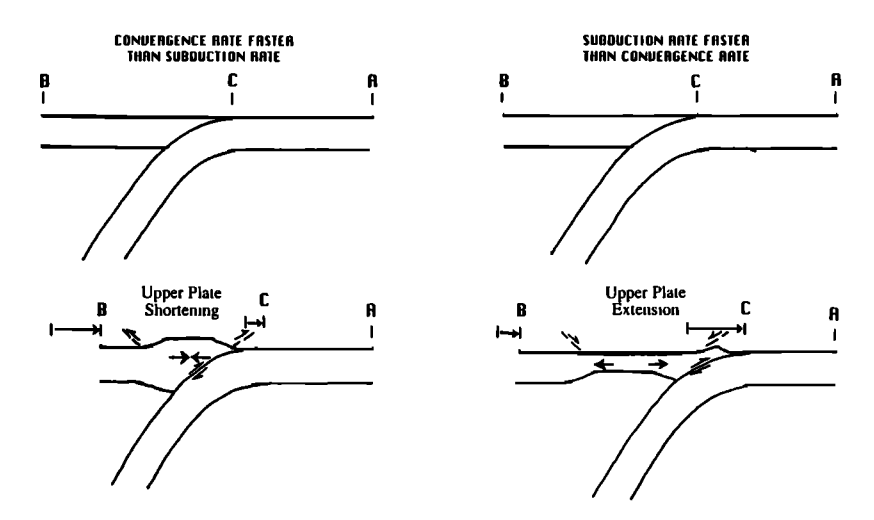


Fig. 1. Schematic diagram illustrating regional deformation of upper plate rocks in response to the relative rates of plate convergence (vector AB) and subduction (vector AC). At advancing plate boundaries (left side) the rate of overall plate convergence is faster than the rate of subduction and the upper plate deforms regionally by horizontal shortening. At retreating plate boundaries (right side) the rate of overall plate convergence is slower than the rate of subduction and the upper plate deforms regionally by horizontal extension.

19449194, 1993, 2, Downloaded from https://agupubs

ominelibrary. wiley.com/doi/10.1029/92TC02248 by University Of British Columbia, Wiley Online Library on [2307/2025]. See the Terms and Conditions (https://onlinelibrary.wiley.com/terms-and-conditions) on Wiley Online Library for rules of use; OA articles are governed by the applicable Creative Commons License

Fig. 2. Generalized locations of Miocene to Quaternary thrust faults and extensional faults within the central Mediterranean region. Locations of profiles 1-3, 5 and 6 are shown in solid lines and approximate locations of cross sections 4A, 4B, and 4C are shown in dashed lines.

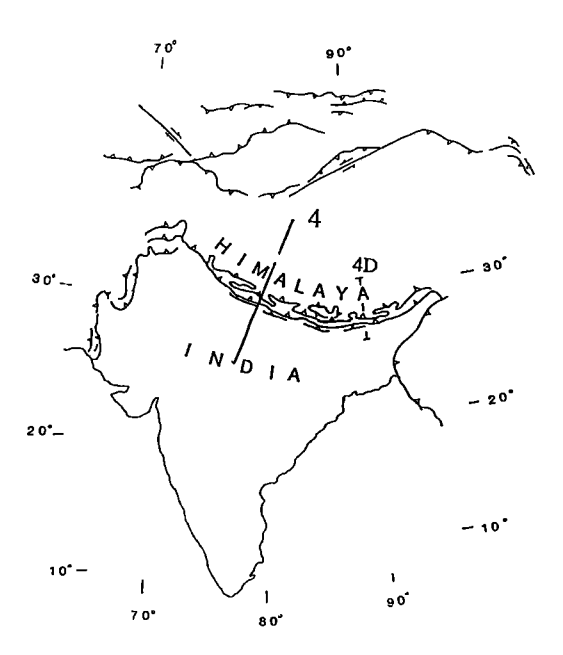


Fig. 3. Generalized locations of major Cenozoic thrust faults within the Himalayan-Tibetan region. Location of profile 4 is shown by a solid line and approximate location of cross section 4D is shown by a dashed line.

foredeep basins and the depth, geometry and age of the foredeep basins are well constrained. The relevant geologic and sedimentary features of each of these thrust belt systems are briefly summarized below and in Table 1 and Figure 4 and are

outlined in more detail, with supporting references, in Appendix B (on microfiche1). The tectonic feature that is most clearly related to the relative rates of convergence and subduction across the retreating subduction boundaries (Apennines, Carpathians and Hellenides) is the presence of regional extension within the overriding plate (Figure 2). Extensional deformation can also be observed locally within orogenic belts formed above advancing subduction boundaries (Alps and Himalayas), but significant regional extension is absent. Instead, regional compression within the overriding plate at these advancing plate boundaries is commonly absorbed by two distinct fold and thrust belts of opposite vergence; a synthetic thrust belt located adjacent to the subducting plate and an antithetic thrust belt located on the opposite side of the topographically high mountains (Figures 2 and 3). Sedimentary basins developed in a back arc position with respect to these advancing orogenic belts are not extensional in origin; instead, they are foredeep basins formed by flexure of the crust beneath the thrust sheets of the antithetic thrust belt.

The orogenic systems developed above advancing and retreating subduction boundaries are also distinguished from one another by a host of other geologic features (Table 1). In general, orogenic systems developed above advancing subduction boundaries are typified by high topographic elevations, large amounts of erosion and denudation, exposure of high-grade metamorphic rocks at the surface, extensive

¹Appendix B is available with entire article on microfiche. Order from the American Geophysical Union, 2000 Florida Avenue, N.W., Washington, D.C. 20009. Document T92-004; \$2.50. Payment must accompany order.

TABLE 1. Generalized Features of Advancing and Retreating Subuction Boundaries in Continental Lithosphere

Generalized Features ^a	Advancing Subductiion Boundaries (Alps, Himalayas) ^b (Retreating Subductiion Boundaries (Apennines, Carpathians, Hellenides) ^b
Regional deformation and structural expressio	Compressional n (antithetic thrust belt)	Extensional ("back arc" basin)
Topographic elevation	High (2 to 6 km) ^c	Low (-3 km to 1 km) ^c
Erosion (denudation)	Great (~30 km)	Minimal (< 5-10 km)
Metamorphism	Medium to high-grade (e.g. kyanite-silimanite-granulite fac	Low grade to none ies) (e.g. greenschist facies)
Deformation of crystalline basement	Deformed to midcrustal depths (faulted-folded-mylonitized)	Mainly undeformed (occasional normal faults)
Postcollisional convergence	Protracted $(tens of millions of years)^d$	Absent or short-lived (a few million years)
Sedimentary facies in foredeep basin	Protracted molasse deposition (following collision)	Protracted flyschs deposition (mainly precollisional to syncollisional)
Geometry of foredeep basin	"Normal" for size of topographic mountains	Anomalously deep for size of topographic mountains
Compensation of foredeep basin	Dominated by topographic loads	Dominated by subduction loads

- a Generalized features only; within individual mountain belts some of these characteristics may be absent or differently developed, depending on age of the belt, lithology, climate, etc.
- b Examples discussed in this paper, supporting references contained in Appendix B.
 c Range for the examples used in this paper. Negative elevations refer to depth below sea level. Because topography was averaged over a 10-km wide swath across the mountains, these average elevations are 1-2 km less than the maximum height of the highest peaks.
 - Current duration in the Alps and Himalayas, which are still undergoing postcollisional convergence.
 - Definition of "collision" is when thick continental crust enters the subduction (thrust belt) system.
 - Coarse clastic, nonmarine to shallow marine deposits.
 - Fine-grained, deepwater submarine fan deposits.

deformation of crystalline basement to midcrustal depths and a protracted history of molasse deposition in front of the advancing orogenic belt (Figure 4). Orogenic systems developed above retreating subduction boundaries are typified by low topographic elevation, little erosion or denudation, lowgrade to no metamorphism, little to no involvement of crystalline basement in shortening and a protracted history of flysch deposition in front of the advancing orogenic belt.

If one defines continental collision as the entry of thick continental crust into the subduction system, then a dramatic difference in postcollisional convergence exists between advancing and retreating subduction boundaries (Table 1 and Appendix B on microfiche). In orogenic belts formed above retreating subduction boundaries, convergence generally ceases shortly after collision when thick portions of the continental crust within the foreland lithosphere enter the subduction zone. For example, the early Miocene history of the Carpathian thrust belt involved subduction of deepwater oceanic or thinned continental crust. When thicker crust of the European plate entered the subduction system in middle Miocene time, the thrust belt became inactive and subduction ceased. Similarly, thrusting ceased in Pliocene-Quaternary time within the Apennines where relatively shallow water portions of the Adriatic foreland have entered the subduction system, but further to the south in Calabria subduction and overthrusting of

the oceanic or thinned continental crust of the Ionian Sea (with a water depth of 2-4 km) is still active. Within the Hellenic subduction system subduction of the deep water Ionian Sea region continues as well. In contrast, orogenic belts formed above advancing subduction boundaries commonly display a protracted history of postcollisional convergence. In the Alps and the Himalayas postcollisional convergence has continued since from Eocene time until the present, lasting for a period of nearly 50 m.y.

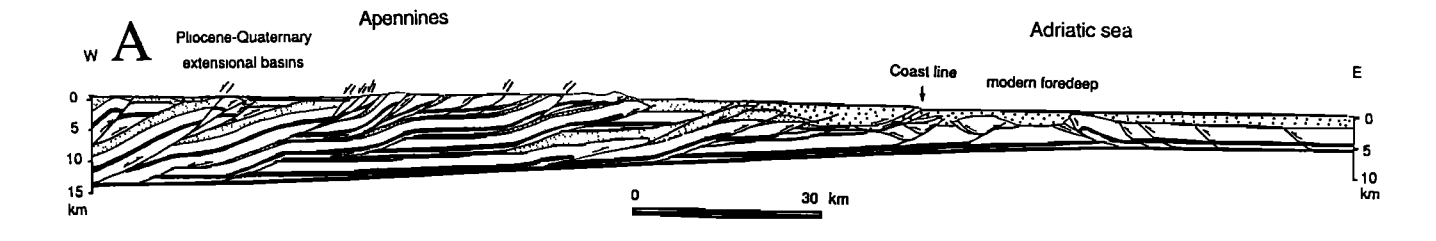
The two types of subduction systems also exhibit important differences in the geometries of the foredeep basins developed adjacent to the orogenic belts, as described in the next section.

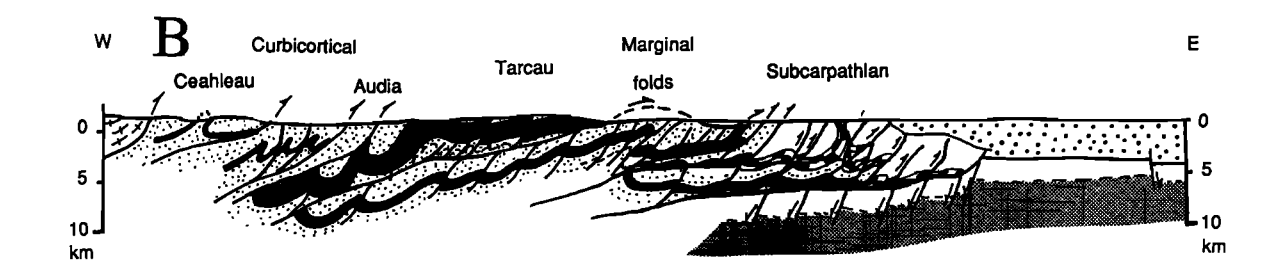
CREATION OF FOREDEEP BASINS BY FLEXURAL LOADING OF THE FORELAND LITHOSPHERE

One of the most important differences between advancing and retreating orogenic systems lies in the relationship between the size of the topographic mountains and the flexural geometry of the adjacent foredeep basins (Figures 5-10). For example, the Himalayan thrust belt, with its average topographic elevation of approximately 6 km, is bordered by a foredeep basin that reaches a maximum depth of about 5 km adjacent to the thrust belt (Figure 8). In contrast, the Apennine thrust belt, with its average topographic elevation of less than 1 km, is bordered by

19449194, 1993, 2, Downloaded from https://agupubs.onlinelibrary.wiley.com/doi/10.102992TC02248 by University Of British Columbia, Wiley Online Library on [2307/2025]. See the Terms and Conditions (https://onlinelibrary.wiley.

and-conditions) on Wiley Online Library for rules of use; OA articles are governed by the applicable Creative Commons License





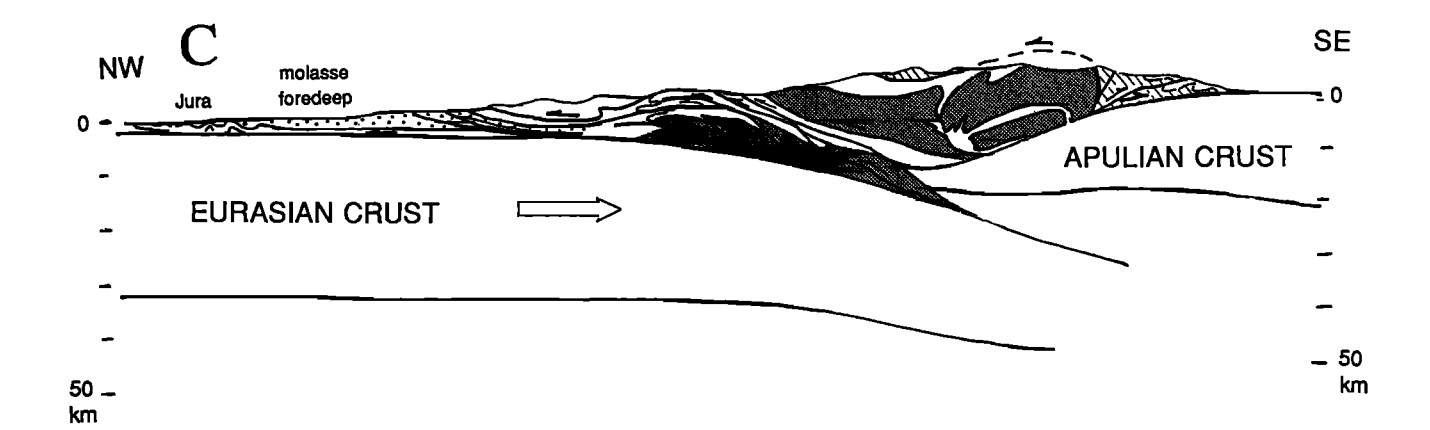


Fig. 4. (a) Cross section through the central Apennines modified from Cooper [1988]. Heavy dots are Pliocene-Quaternary deposits in the modern foredeep basin and in the extensional basins of the western Apennines. Fine dots are Apennine flysch. Thick solid line is the stratigraphic level of the Triassic evaporites. Note that thrust sheets involve Mesozoic and, rarely, Paleozoic sedimentary rocks of the foreland, but do not involve crystalline basement. (b) Cross section through the East Carpathians modified after Paraschiv [1979]. Heavy dots are Miocene-Quaternary deposits in the modern foredeep basin. Finely dotted, black and checkered units are Carpathian flysch. Shaded area represents Triassic and older rocks of the European foreland. Crosses (west end of profile) are crystalline rocks deformed and thrust in Cretaceous time. Note that thrust sheets do not involve Paleozoic or crystalline rocks of the foreland. (c) Cross section through the Western and Southern Alps modified after Trümpy [1980] and Roure et al. [1990]. Heavy dots are Oligo-Miocene molasse of the modern foredeep basin and contained within the outer nappes. Shaded areas represent crystalline basement rocks of the Eurasian plate and basement fragments in the Pennine zone that are involved in alpine deformation. (d) Schematic cross section through the central Himalaya, greatly modified from Gansser [1964]. Heavy dots are Miocene-Quaternary molasse of the modern foredeep basin and contained within the outer thrust sheets of the Siwaliks. Light shading represents low-grade metamorphic rocks of the Lesser Himalaya. Dark shading represents high-grade rocks of the High Himalayan crystalline zone. Unshaded area represents Paleozoic to Lower Tertiary sedimentary rocks of the Tibetan zone and Cretaceous forearc deposits of the Xigatze Group (the latter rest on an ophiolitic basement shown in black.) Approximate locations of profiles shown in Figures 2 and 3.

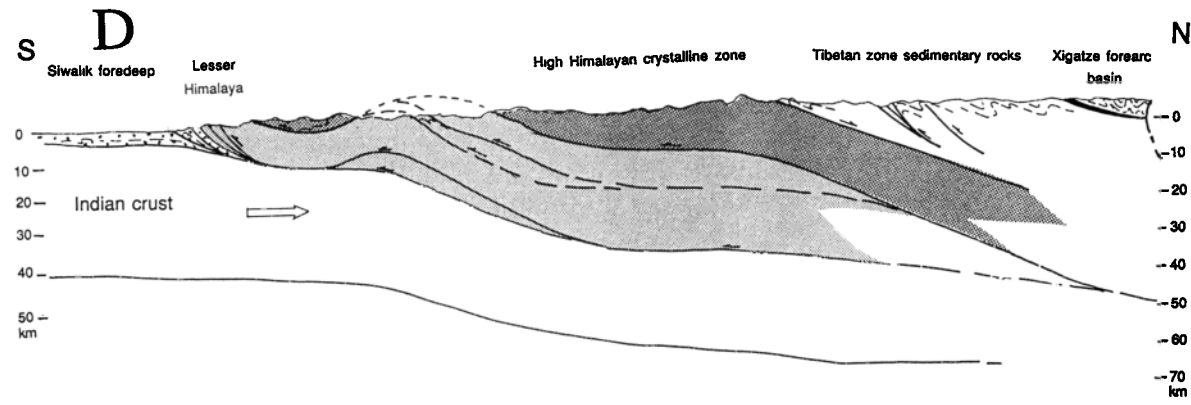


Fig.4 (continued)

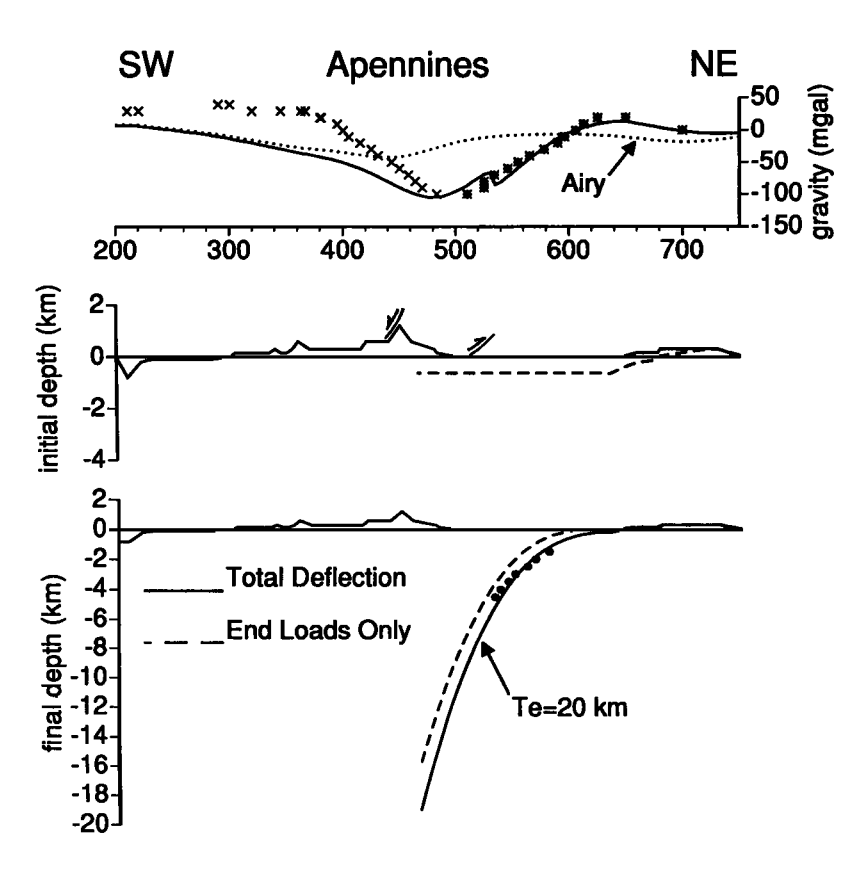


Fig. 5. Observed and computed flexure for profile 1 (Apennines). (Top) Symbols show observed Bouguer gravity anomalies; solid symbols are observations used explicitly in computing the best fitting flexural profile. Solid line shows computed Bouguer anomalies corresponding to best fitting deflection profile. Dotted line shows Bouguer anomalies that would be expected if topography were Airy compensated. (Middle) Dashed line shows initial (preflexural) topography or bathymetry corresponding to the best fitting flexural profile. Solid line shows present-day topography. Approximate positions of thrust front and extensional front also shown. (Bottom) Symbols show observed depth of the foredeep basin. Solid curve shows best fitting flexural profile. Dashed curve shows the component of flexural profile due to subsurface (subduction) loads.

a foredeep basin that reaches a maximum depth of more than 8 km (Figure 5). Only part of this discrepancy can be ascribed to differences in the flexural strength of the foreland lithospheres. Of greater importance is the relationship between emplacement

of thrust sheets and loading of the foreland lithosphere. Because the source of loading responsible for flexure of the foreland lithosphere is directly related to fundamental differences in the tectonic setting of advancing and retreating 19449194, 1993, 2, Downloaded from https://agupubs.onlinelibrary.wiley.com/doi/10.1029/92TC02248 by University Of British Columbia, Wiley Online Library on [23.07/2025]. See the Terms and Conditions

/onlinelibrary.wiley.com/terms-and-conditions) on Wiley Online Library for rules of use; OA articles are governed by the applicable Creative Commons Licensee

19449 194, 1993, 2, Downloaded from https://agupubs.onlinelibrary.viley.com/doi/10.1029/92TC02248 by University Of British Columbia, Wiley Online Library on [23.07/2025]. See the Terms and Conditions (https://onlinelibrary.viley.com/terms-and-conditions) on Wiley Online Library for rules of use; OA arctles are governed by the applicable Creative Commons Licensea

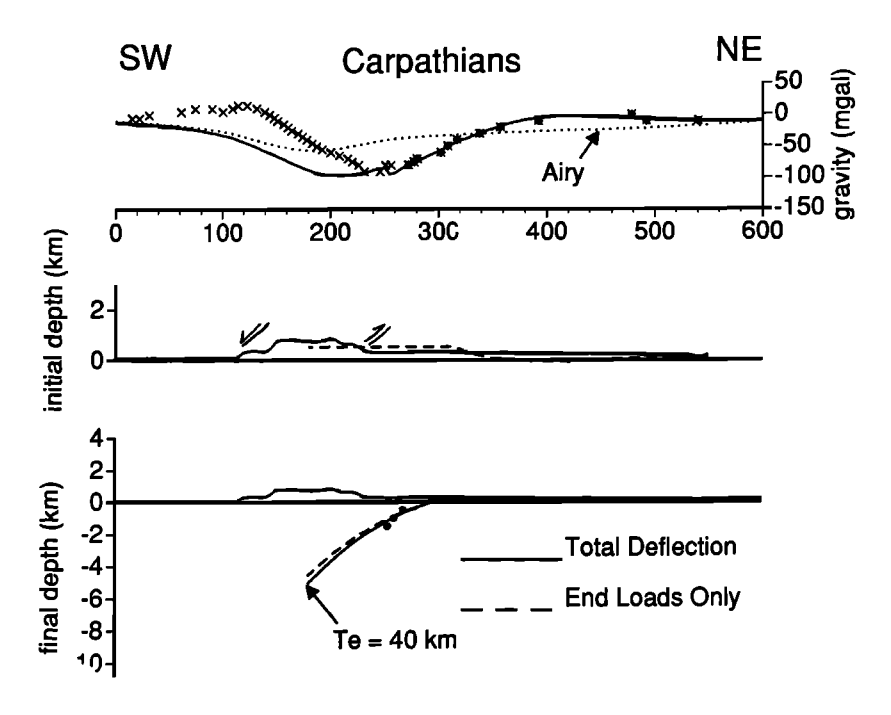


Fig. 6. Observed and computed flexure for profile 2 (Carpathians). (Top) Symbols show observed Bouguer gravity anomalies; solid symbols are observations used explicitly in computing the best fitting flexural profile. Solid line shows computed Bouguer anomalies corresponding to best fitting deflection profile. Dotted line shows Bouguer anomalies that would be expected if topography were Airy compensated. (Middle) Dashed line shows initial (preflexural) topography or bathymetry corresponding to the best-fitting flexural profile. Solid line shows present-day topography. Approximate positions of thrust front and extensional front also shown. (Bottom) Symbols show observed depth of the foredeep basin. Solid curve shows best fitting flexural profile. Dashed curve shows the component of flexural profile due to subsurface (subduction) loads.

subduction boundaries, and to the driving mechanisms for subduction and convergence, this topic is examined here in some detail.

Deflection and Gravity Profiles

Profiles of Bouguer gravity anomalies, topography and bathymetry, and foredeep basin geometry were constructed across each orogenic belt (Figures 5-10). Basin geometries were constrained by the depth to the base of the oldest sedimentary strata that form a part of the modern foredeep basins, as follows. profile 1 (Apennines), depth to base Pliocene; profile 2 (Carpathians), depth to base Miocene; profile 3 (Hellenides), no depth data available; profile 4 (Himalayas), depth to base Mio-Pliocene; profile 5 (Eastern and Southern Alps), depth to base Miocene (northern basin) and depth to base Pliocene (?) (southern basin); profile 6, (Western and Southern Alps and northern Apennines), depth to base Miocene. Deflection data were obtained from Vurov et al. [1986], Pieri and Groppi [1981], E. Patacca and P. Scandone, unpublished data [1985], Lyon-Caen and Molnar [1985, 1989], Kollmann and Malzer [1980], Beck-Mannagetta and Matura [1980], Fuchs [1980] and Karunakaran and Rao [1976].

Bouguer gravity data were compiled from published cross sections and contour maps [Ogniben et al., 1975; Morelli et al. 1969, 1975; Lyon-Caen and Molnar, 1985, 1989; Tomek et al., 1988; Schweizerische Geophysikalische Kommission, 1979; Bureau Gravimetrique International, 1962-1963, 1964-1965;

Intergovernmental Oceanographic Commission, 1989]. Across topographically high regions in the Western Alps (Profile 6) and the Himalayas (profile 4) we used terrain-corrected measurements from Lyon-Caen and Molnar [1985, 1989]. Gravity data from topographically high parts of the Eastern Alps were not terrain corrected because the original gravity measurements were not available. Hence Bouguer gravity anomalies that are more negative than about 140 mGal are probably biased and were not used when solving for the flexural geometry of the foreland lithosphere. The maximum elevations crossed by profiles 1, 2 and 3 (Apennines and Carpathians) are about 1 km or less, so we judged terrain corrections to be unnecessary.

Flexural Analysis: Method

The present depth of each foredeep basin in profiles 1-6 is the result of the net deflection of the underlying foreland lithosphere from some initial (preflexural) depth $w_{in}(x)$ to its final depth w(x) (Figure 11) Flexural modeling of the net deflection $[w(x)-w_{in}(x)]$ can therefore be used to examine the flexural strength of the underlying lithosphere and the loads that act on that lithosphere to produce the observed deflection. Gravity data also provide important constraints on the initial depth $w_{in}(x)$ and the general geometry of the subducted lithosphere beneath the thrust belt where direct observations of flexure cannot be made. The method employed here is an expansion of techniques developed for bending of a thin elastic

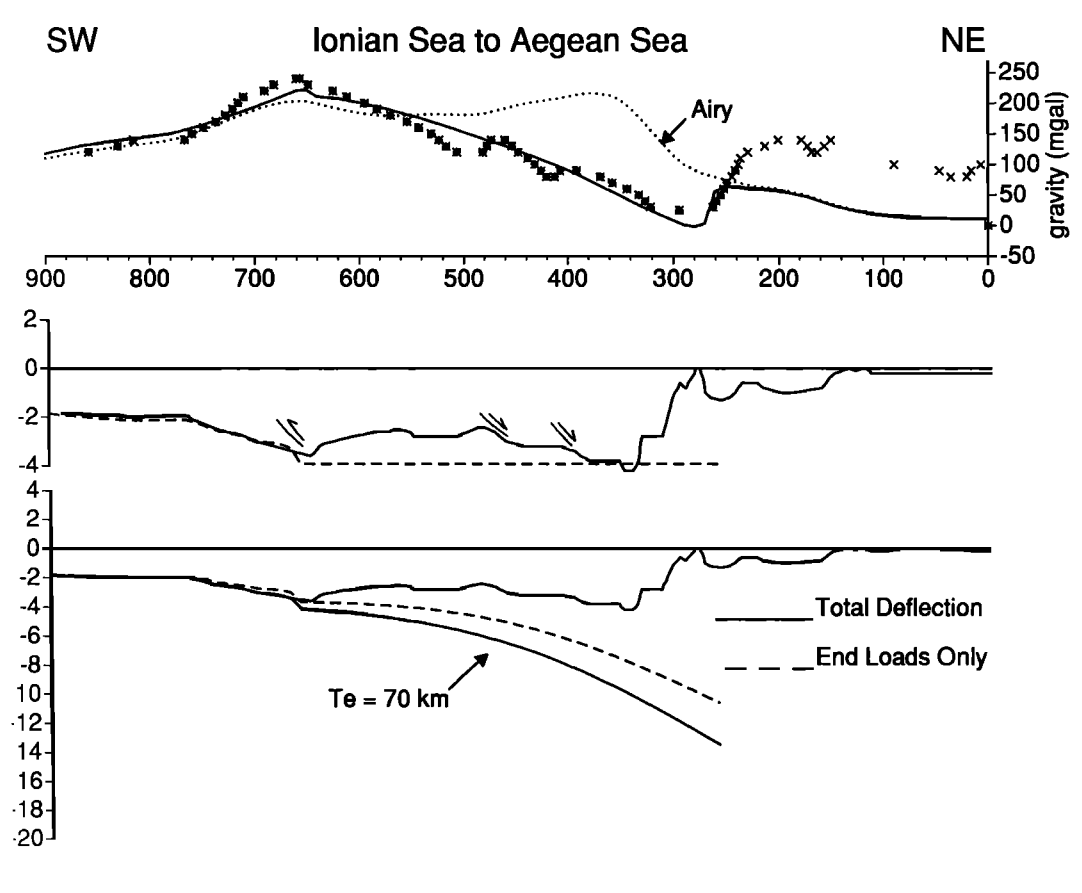


Fig. 7. Observed and computed flexure for Profile 3 (southern Hellenides). Top: Symbols show observed Bouguer gravity anomalies; solid symbols are observations used explicitly in computing the best fitting flexural profile. Solid line shows computed Bouguer anomalies corresponding to best fitting deflection profile. Dotted line shows Bouguer anomalies that would be expected if topography were Airy compensated. Middle: Dashed line shows initial (preflexural) topography or bathymetry corresponding to the best fitting flexural profile. Solid line shows present-day topography. Approximate positions of thrust front and extensional front also shown. Bottom: Symbols show observed depth of the foredeep basin. Solid curve shows best fitting flexural profile. Dashed curve shows the component of flexural profile due to subsurface (subduction) loads.

sheet by Royden [1988b], Moretti and Royden [1988] and Kruse [1989] for loading of an elastic foreland lithosphere, and solves simultaneously for the initial depth and the net deflection from basin depth and gravity data. The mathematical basis for this method is described in detail by S.E. Kruse and L.H. Royden ("Bending and unbending of an elastic lithosphere: The Cenozoic history of the Apennine and Dinaride foredeep basins, submitted to *Tectonics*, 1992).

After the flexural model that provides the best fit to the observed depth and gravity data has been computed for each profile, the total deflection can be divided into two parts: the deflection due to topographic loads and the deflection due to subsurface loads (Figure 11). In this paper the topographic load is defined as the load created by all material, basin sediments or thrust sheets, present above the initial (preflexural) depth of the surface of the foreland lithosphere (minus the load of any water that was initially present between the initial depth and sea level). The subsurface load is defined as any other loads acting on the foreland lithosphere that are not expressed as

surface topography. The deflection due to both of these loads is flexurally amplified by the weight of infilling material present below the initial (preflexural) depth and above the final (postflexural) depth of the surface of the foreland lithosphere. This is essentially the familiar "sediment loading term" used in analysis of extensional sedimentary basins, except that here the infilling material may consist either of basin sediments or thrust sheet material.

19449194, 1993, 2, Downloaded from https://agupubs.onlinelibrary.wiley.com/doi/10.1029/92TC02248 by University Of British Columbia, Wiley Online Library on [2307/2025]. See the Terms and Conditions (https://agupubs.onlinelibrary.wiley.com/doi/10.1029/92TC02248 by University Of British Columbia, Wiley Online Library on [2307/2025]. See the Terms and Conditions (https://agupubs.onlinelibrary.wiley.com/doi/10.1029/92TC02248 by University Of British Columbia, Wiley Online Library on [2307/2025]. See the Terms and Conditions (https://agupubs.onlinelibrary.wiley.com/doi/10.1029/92TC02248 by University Of British Columbia, Wiley Online Library on [2307/2025]. See the Terms and Conditions (https://agupubs.onlinelibrary.wiley.com/doi/10.1029/92TC02248 by University Of British Columbia, Wiley Online Library on [2307/2025]. See the Terms and Conditions (https://agupubs.onlinelibrary.wiley.com/doi/10.1029/92TC02248 by University Of British Columbia, Wiley Online Library on [2307/2025]. See the Terms and Conditions (https://agupubs.onlinelibrary.wiley.com/doi/10.1029/92TC02248 by University Of British Columbia, Wiley Online Library.wiley.com/doi/10.1029/92TC02248 by University Online Library.wiley.com/doi/10.1029/92TC02248 by

//onlinelibrary.wiley.com/terms-and-conditions) on Wiley Online Library for rules of use; OA articles are governed by the applicable Creative Commons License

In computing results for profiles 1-6, the subsurface load has been equated with the terminal bending moment and vertical shear force that act at the effective plate end to maintain the observed plate flexure (Figure 11). Thus these subsurface loads contribute to the computed flexure of the foreland lithosphere (via the terminal forces and moments) but do not contribute to the computed gravity anomalies (except insofar as they affect the deflection of the lithosphere). The portion of the deflection that is due to subsurface loading (including amplification by infilling material) can be computed by applying the terminal bending moment and vertical shear force to the

19449194, 1993, 2, Downloaded from https://agupubs

onlinelibrary.wiley.com/doi/10.1029/92TC02248 by University Of British Columbia.

Wiley Online Library on [23/07/2025]. See

ons) on Wiley Online Library for rules of use; OA articles are governed by the applicable Creative Commons

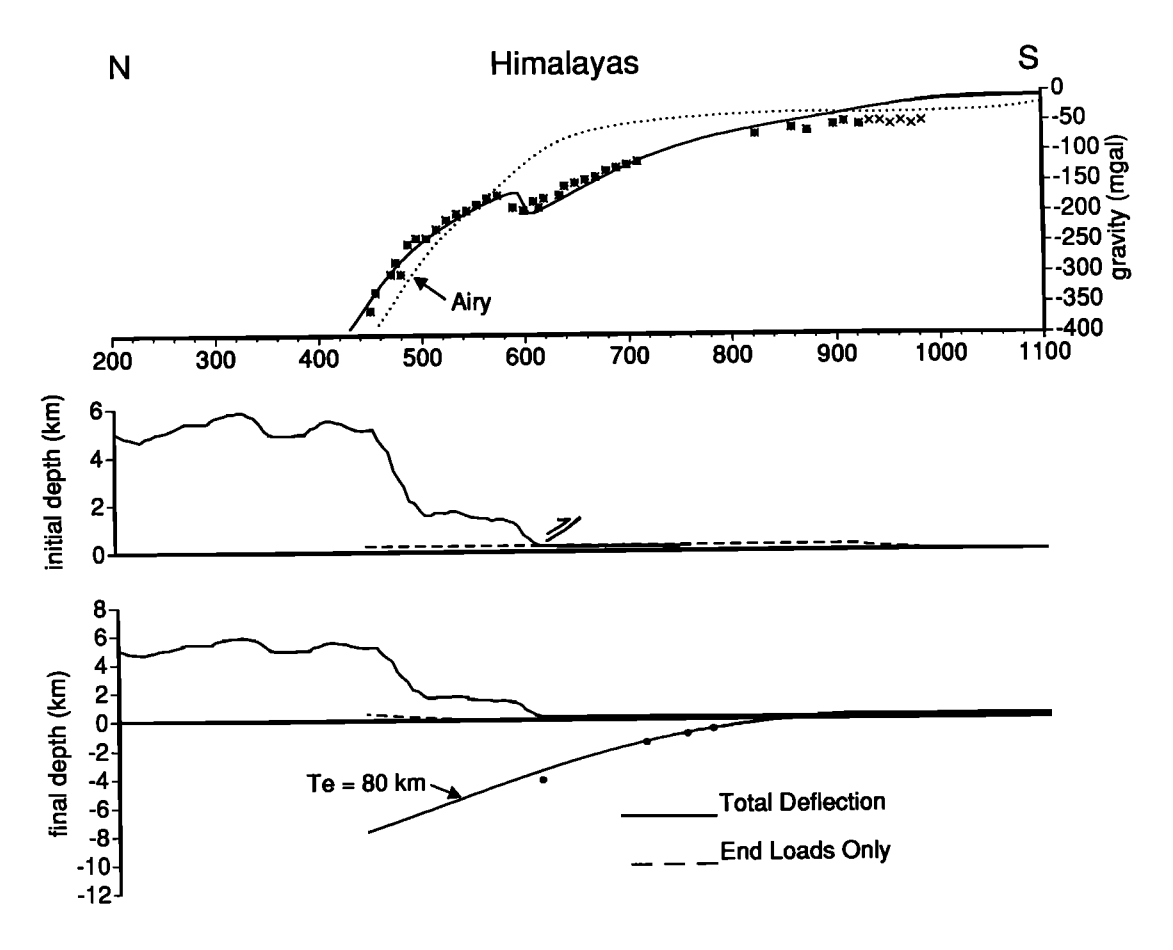


Fig. 8. Observed and computed flexure for profile 4 (Himalayas). (Top) Symbols show observed Bouguer gravity anomalies; solid symbols are observations used explicitly in computing the best fitting flexural profile. Solid line shows computed Bouguer anomalies corresponding to best fitting deflection profile. Dotted line shows Bouguer anomalies that would be expected if topography were Airy compensated. (Middle) Dashed line shows initial (preflexural) topography or bathymetry corresponding to the best fitting flexural profile. Solid line shows present-day topography. Approximate positions of thrust front also shown. (Bottom) Symbols show observed depth of the foredeep basin. Solid curve shows best fitting flexural profile. Dashed curve shows the component of flexural profile due to subsurface (subduction) loads.

effective plate end in the absence of a topographic load. (If the surface of the plate is flexed above its initial elevation, it is assumed that nothing was deposited on or eroded from the uplifted area.) Subtracting the deflection due only to the subsurface loads from the total plate deflection yields the deflection due only to the topographic loads (including amplification by infilling material).

Analysis of profiles 1-4 is straightforward because each of these profiles corresponds to simple one-sided subduction of the foreland lithosphere beneath the adjacent mountain belt (Figures 5-8). Along profile 5 where the European lithosphere has been subducted southward beneath the Eastern Alps and the Adriatic lithosphere has been subducted northward beneath the Southern Alps, each foreland was treated as a broken plate subject to one-sided subduction. The breaks were assumed to coincide spatially (Figure 9) but no stress was transmitted from one plate end to another. Along profile 6 the European lithosphere has been subducted southward beneath the Western

Alps and the Adriatic lithosphere has been subducted northward beneath the Southern Alps and southward beneath the Apennines. In this case the European foreland was treated as a broken plate subject to one-sided subduction, while the Adriatic lithosphere was treated as a doubly broken plate subject to two-sided subduction. Horizontal compressional stresses were neglected along all profiles.

Flexural Analysis: Results

The computed best fitting deflections, Bouguer gravity anomalies and initial water depths for profiles 1-6 are shown in Figures 5-10. (Values of end-load, end-moment, flexural rigidity, etc., for each of these profiles are given in Table 2.) In general, the fit between observed and computed values is quite good on all profiles except over the back arc region behind the Apennine, Carpathian and Hellenide thrust belts, where the observed Bouguer anomalies are more positive than the

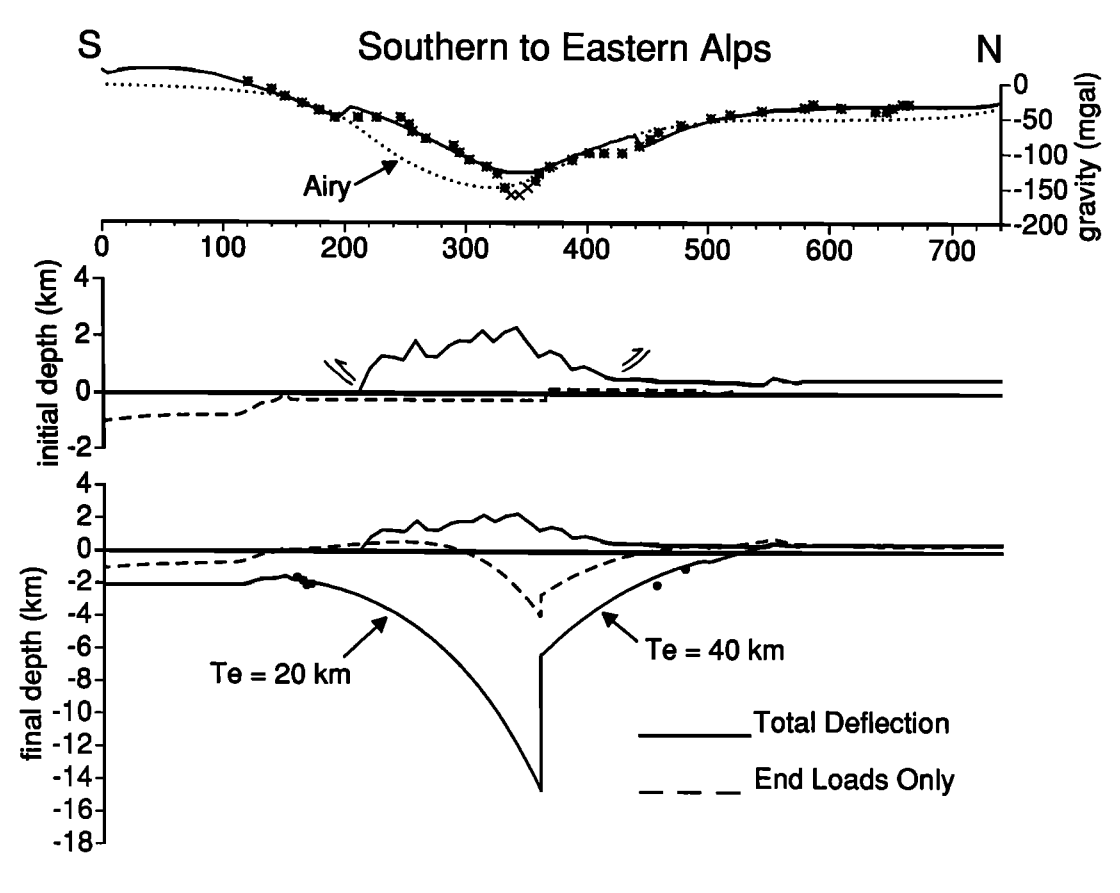


Fig. 9. Observed and computed flexure for profile 5 (Southern to Eastern Alps). (Top) Symbols show observed Bouguer gravity anomalies; solid symbols are observations used explicitly in computing the best fitting flexural profile. Solid line shows computed Bouguer anomalies corresponding to best fitting deflection profile. Dotted line shows Bouguer anomalies that would be expected if topography were Airy compensated. (Middle) Dashed line shows initial (preflexural) topography or bathymetry corresponding to the best fitting flexural profile. Solid line shows present-day topography. Approximate positions of thrust fronts also shown. (Bottom) Symbols show observed depth of the foredeep basin. Solid curve shows best fitting flexural profile. Dashed curve shows the component of flexural profile due to subsurface (subduction) loads.

computed anomalies by 50-100 mGal over a region at least several hundred kilometers wide. The effective elastic plate thicknesses determined for these best fit profiles are very similar to those found by other authors for the same orogenic belts [Royden and Karner, 1984; Royden, 1988b; Lyon Caen and Molnar, 1983, 1985, 1989, Karner and Watts, 1983].

Figures 5-10 also show the component of deflection due only to the subsurface load along each profile (see also Table 2). For example, Figure 8 shows that subsurface loads acting on the Indian lithosphere beneath the Himalayas are responsible for virtually none of the deflection and loading of the Indian foreland. Thus the depth and flexural shape of the foreland basin are entirely the result of loading of the foreland lithosphere by advancing thrust sheets and are consistent with the size of the mountain belt adjacent to the basin and the flexural rigidity of the foreland lithosphere. In contrast, the Apennine foredeep basin looks quite different (Figure 5); subsurface loads acting on the Adriatic lithosphere beneath the Apennines are responsible for almost all of the deflection and loading of the Adriatic foreland. The topographic load

represented by the size of the adjacent mountain belt contributes only negligibly to the flexure of the lithosphere beneath the basin. The deflection of the Carpathian foreland lithosphere also appears to be controlled almost completely by subsurface loads acting on the subducted lithosphere beneath the thrust belt (Figure 6). (A discussion of possible sources of error in determining subsurface loads is given in Appendix A.)

19449194, 1993, 2, Downloaded from https://agupubs

onlinelibrary.wiley.com/doi/10.1029/92TC02248 by University Of British Columbia, Wiley Online Library on [23/07/2025]. See the Terms

ons) on Wiley Online Library for rules of use; OA articles are governed by the applicable Creative Commons

The deflection of the foreland lithosphere beneath and in front of the Hellenides is dominantly controlled by large subsurface loads, which are a factor of 3 to 4 times larger than the subsurface loads acting beneath the Apennines (Figure 7 and Table 2). There is also a nonnegligible contribution from the topographic load that is due not to the presence of topographically high mountains but rather to the elevation difference between the foreland (at 4 km below sea level) and the overriding plate (roughly at sea level). Thus a large increase in elevation going from the foreland to the overriding plate can produce a large topographic load even without the production of topographically high mountains. However, the effects of subsurface loading still predominate along this profile.

19449194, 1993, 2. Downloaded from https://agupubs.onlinelibrary.wiley.com/doi/10.1029/92TC02248 by University Of British Columbia, Wiley Online Library on [23/07/2025]. See the Terms

ns) on Wiley Online Library for rules of use; OA articles are governed by the applicable Creative Commons

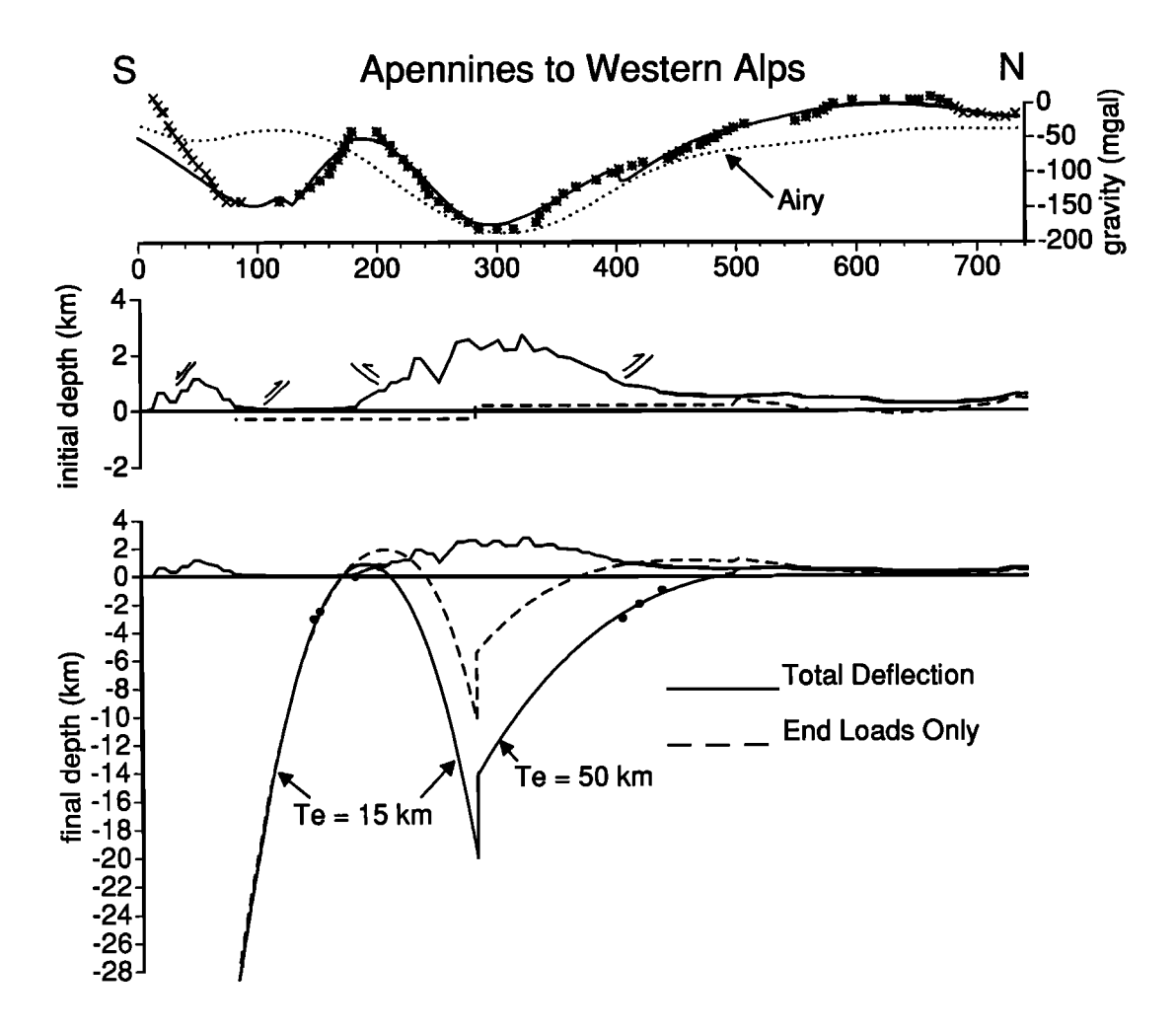
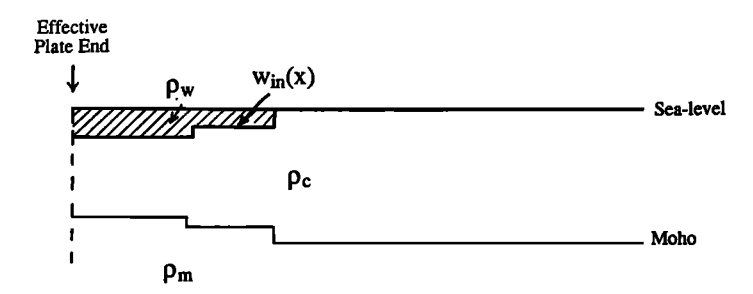


Fig. 10. Observed and computed flexure for profile 6 (Apennines to Western Alps). (Top) Symbols show observed Bouguer gravity anomalies; solid symbols are observations used explicitly in computing the best fitting flexural profile. Solid line shows computed Bouguer anomalies corresponding to best fitting deflection profile. Dotted line shows Bouguer anomalies that would be expected if topography were Airy compensated. (Middle) Dashed line shows initial (preflexural) topography or bathymetry corresponding to the best fitting flexural profile. Solid line shows present-day topography. Approximate positions of thrust fronts and extensional front also shown. (Bottom) Symbols show observed depth of the foredeep basin. Solid curve shows best fitting flexural profile. Dashed curve shows the component of flexural profile due to subsurface (subduction) loads.

Compensation of the foreland(s) in front of the Alps is due to both subsurface loading and topographic loading (Figures 9 and 10). The topographic loading is responsible for most of the deflection of the foreland lithosphere in front of the mountain belt (as opposed to the deflection beneath the mountain belt). In fact, the subsurface loads actually cause uplift of the foreland basement beneath the foredeep basins on the north and south side of the Alps, and only cause subsidence beneath in internal parts of the thrust belt. Thus the observed depths of the foreland basins in front of the northern and southern sides of the Alps are actually shallower than would be expected from the topographic loads alone, while the computed depths of the subducted plates beneath the internal parts of the mountains are deeper than would be expected from the topographic loads alone.

The contrast between loading by topographic loads and loading by subsurface loads is illustrated particularly well in profile 6, where it crosses the intermediate foreland between the north vergent Apennine thrust belt and the south vergent Southern Alps (Figures 2 and 10). The topographic elevation of the Apennines is much less than that of the Alps, but across its entire width the intermediate foreland basin between the Apennines and the Alps deepens southward toward the Apennines. Examination of the contribution of topographic and subsurface loads to the deflection of the foreland shows that the subsidence of the southern end of the Adriatic plate beneath the Apennines is entirely due to the presence of large subsurface loads beneath the Apennines; the topographic load of the Apennines contributes almost nothing to the deflection. Thus the southward deepening asymmetry of the intermediate



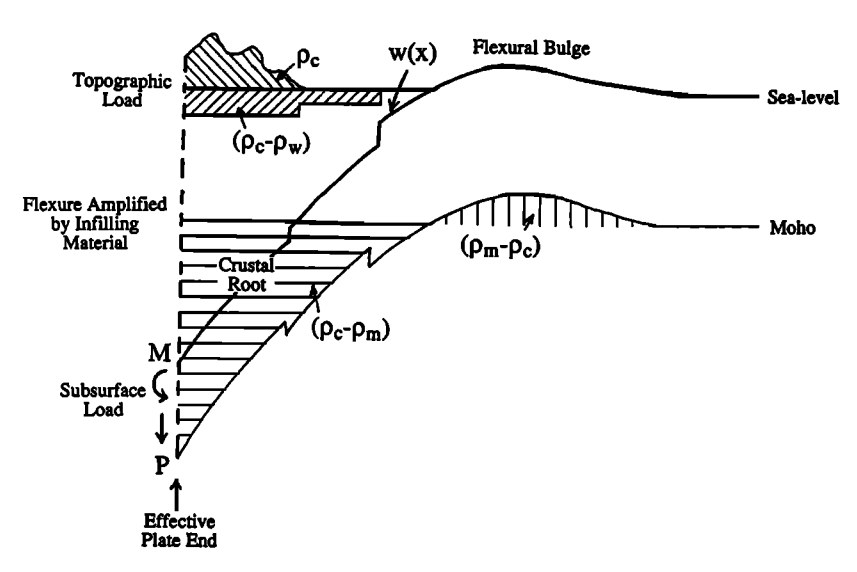


Fig. 11. Schematic plate geometry (top) before and (bottom) after flexure in the simplified case where basin sediments have the same density as the crust. Prior to flexure and subduction the foreland lithosphere is assumed to be in Airy isostasy with an initial bathymetry (or topography) $w_{in}(x)$. Densities are as shown: density of water, ρ_w , density of crust, ρ_c , and density of mantle, ρ_m . After flexure and overthrusting, the depth to the top of the flexed plate is w(x). Loads acting on the foreland lithosphere are: (1) the topographic load, shown by diagonally hatched lines (load added to the plate has density ρ_c above sea-level and density $(\rho_c - \rho_w)$ below sea-level); (2) the subsurface load, represented by a bending moment M and a vertical shear force P at the effective plate end; and (3) the infilling material present below $w_{in}(x)$ and above w(x), and with density ρ_c . In this simple example where the density of the basin sediments is the same as ρ_c , the only contributions to the Bouguer gravity are a positive mass anomaly with density contrast $(\rho_m - \rho_c)$ under the flexural bulge and a negative mass anomaly with density contrast ($\rho_c - \rho_m$) corresponding to the crustral root beneath the mountains.

foreland basin occurs primarily in response to subsurface loads acting on the Adriatic lithosphere beneath the Apennines. This has resulted in a foreland basin whose geometry has little relation to the size of the adjacent mountain belts.

Summary

In general, it appears that foredeep basins that form in front of advancing subduction zones, such as the Alps and the Himalayas, are mainly compensated by topographic loads equivalent to the topographic elevation of the adjacent thrust belts, although subsurface loads may play a lesser role. In contrast, foredeep basins that form in front of retreating

subduction zones, such as the Apennines, the Carpathians and the Hellenides, appear to be largely compensated by subsurface loads acting on the downgoing lithosphere; topographic loads equivalent to the topographic elevation of the adjacent thrust belts plays a lesser, sometimes negligible, role in loading of the foreland lithosphere. End-member examples of foredeep basin geometry are provided by the Apennine and Carpathian foredeep basins on one hand and Himalayan foredeep basin on the other hand because the former are compensated almost completely by subsurface loads acting on the subducting plates while the latter is compensated almost completely by topographic loads associated with the emplacement of thrust sheets onto the foreland.

19449194, 1993, 2, Downloaded from https://agupubs.onlinelibrary.wiley.com/doi/10.1029/92TC02248 by University Of British Columbia, Wiley Online Library on [23/07/2025]. See the Terms

onditions) on Wiley Online Library for rules of use; OA articles are governed by the applicable Creative Commons License

19449194, 1993, 2, Downloaded from https://agupub

onlinelibrary.wiley.com/doi/10.1029/92TC02248 by University Of British Columbia, Wiley Online Library on [23/07/2025]. See the Terms

and Conditions (https

conditions) on Wiley Online Library for rules of use; OA articles are governed by the applicable Creative Common

TABLE 2. Flexural Parameters, Loads and Densities Used on Profiles 1-6a

	Profile 1	Profile 2	Profile 3	Profile 4	Profi	ile 5 ^b		Profile 6b	
	Apennines	Carpathians	Hellenides	Himalayas	Eastern Alps	Southern Alps	Western Alps	Southern Alps	Apennines
Effective elastic plate thickness (km)	20	40	70	80	40	20	50	15	15
Flexural rigidity (Nm)	5.7×10 ²²	4.6×10 ²³	2.8×10 ²⁴	3.7×10 ²⁴	4.6×10 ²³	1.9×10 ²³	9.0×10 ²³	2.4×10 ²²	2.4×10 ²²
Position of effective plate ends (km) ^c	465	180	260	440	360	360	280	280	80
Vertical shear force at plate end (N/m) ^d	-2.1×10 ¹²	-0.8×10 ¹²	-6.0×10 ¹²	+1.9×10 ¹²	+0.9×10 ¹²	+2.2×10 ¹²	+3.6×10 ¹²	+2.3×10 ¹²	-4.7×10 ¹²
Bending moment at plate end (N/m) ^e	1.1×10 ¹⁷	1.8×10 ¹⁷	0.8×10 ¹⁷	3.4×10 ¹⁷	2.5×10 ¹⁷	3.2×10 ¹⁷	9.0×10 ¹⁷	2.5×10 ¹⁷	-1.0×10 ¹⁷
Position of inner edge of foredeep basin (km) ^c	532	254	480	400	442	550	403	125	180
Sediment density in foredeep basin (kg/m ³) ^f	2300 2400 2500 2600 2700	2400 2400 2400 2400 2400	2100 2200 2400 2500 2600	2400 2400 2400 2400 2400	2400 2500 2500 2500 2500	2400 2500 2500 2500 2500	2400 2500 2500 2500 2500	2400 2500 2500 2500 2500	2400 2500 2500 2500 2500

^a As shown in Figures 5-10.

b These profiles involve subduction of more than one foreland region; see text and Figures 9 and 10.

c Relative to coordinates shown in Figures 5-10.

Megative values are downward force.

Positive values correspond to concave downward curvature.

f Sediment densities for sediments in the upper 5 km of the foredeep basins. The top value corresponds to the density of the upper 1 km of sediment (relative to the sediment surface), the second value refers to the underlying kilometer of sediment, etc. Elsewhere, the density of the infilling material and the crust were assumed to be 2670 kg/m³ and the density of the mantle was assumed to be 3200 kg/m³.

POSSIBLE SOURCES FOR SUBSURFACE LOADS AT SUBDUCTION BOUNDARIES

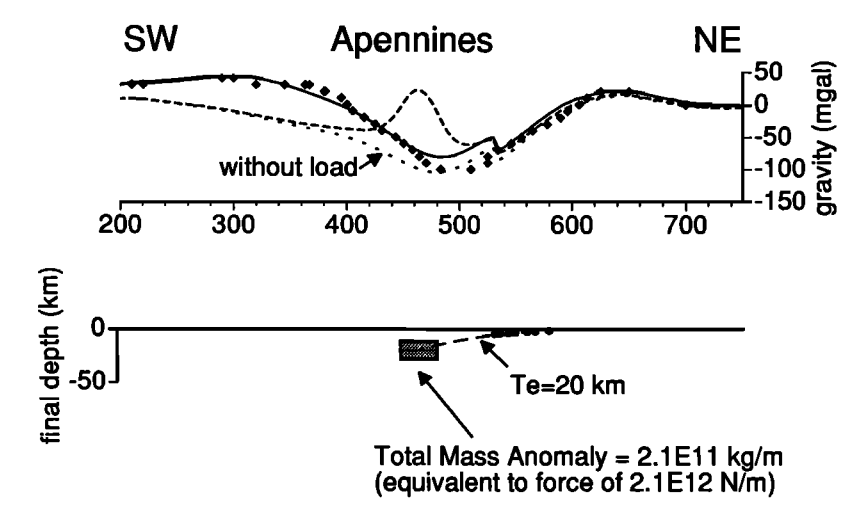
Emplacement of Ultramafic Bodies

A number of authors have proposed that subsurface loads result from anomalously dense material (ultramafic bodies) emplaced onto the foreland lithosphere at depth (for example in the internal parts of the Western Alps, Karner and Watts [1983]. Beneath the Apennines, Carpathians and Hellenides the size of the vertical shear force needed on the end of the plate is between 0.8×10¹² and 6.0×10¹² N/m (Table 2), requiring an ultramafic body with a cross-sectional area of 160 to 1300 km² along the entire length of the belt (assuming that the density of the ultramafic material is 500 kg/m³ greater than the surrounding crustal material). This is unreasonably large and indicates that the presence of ultramafic bodies at depth is not responsible for the subsurface loads in these orogenic belts. A body of this size and density at crustal depths should also generate an obvious short-wavelength positive gravity anomaly. For example, Figures 12-14 illustrate the gravity anomalies that would result if the subsurface loads required to maintain flexure along profiles 1-3 (through the Apennines, Carpathians and Hellenides) were attributed to an ultramafic body with a density 500 kg/m³ greater than the surrounding material. The

ultramafic body has been assumed to be 14 km thick and centered on the effective plate ends (at about 20, 6 and 15 km depth, respectively). The resulting gravity anomalies are unmistakable, yielding pronounced narrow gravity highs that are not present in the observed gravity data. This further indicates that the subsurface loads required to maintain the deflection of the foreland lithosphere beneath the Apennines, Carpathians and Hellenides cannot be attributed to excess mass at crustal depths.

Overthrusting of a Deepwater Continental Margin

Other authors have suggested that apparent subsurface loading is the result of overthrusting of a continental margin so that the deepwater portion of the margin is present beneath the inner parts of the thrust belt, while only shallower water parts of the margin are observable beneath the external parts of the thrust belt and in the foreland [Stockmal and Beaumont, 1987]. As Stockmal and Beaumont [1987] point out, if the initial shallow water conditions are extrapolated back beneath the thrust belt, one will significantly underestimate the size of the topographic load present and may erroneously assume that a large subsurface load must be present beneath the thrust belt. Figure 15 shows the best fit flexural solution that is obtained for the Apennines by fixing the initial water depth at 3 km beneath



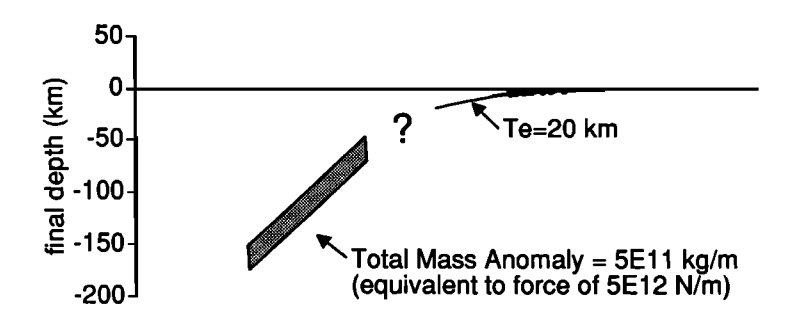


Fig. 12. (Top) Observed (symbols) and computed gravity anomalies across profile 1 (Apennines) assuming that the subsurface load corresponds to a midcrustal mass anomaly (dashed line) or to a dense subducted slab at depth (solid line). Dotted line shows computed Bouguer anomalies corresponding to the best fitting deflection profile without accounting for the mass of the subsurface load. (Middle) Size and position of inferred midcrustal mass anomaly with a density contrast of 500 kg/m³. (Bottom) Inferred size and position of dense subducted slab dipping 45° and extending from 50 to 170 km depth.

the thrust belt, but solving for the best fitting initial water depth elsewhere. The deflection due to subsurface loading is mostly unchanged by this assumption and the vertical shear force acting on the plate end is reduced only by about 5%, from -2.1×10¹² N/m to -2.0×10¹² N/m. Thus it is clear that overthrusting of deep water portions of the foreland lithosphere cannot be responsible for the subsurface loads present beneath the Apennine thrust belt. Similar results can be obtained for the Carpathian and Hellenide belts.

Dense Subducted Slab at Subcrustal Depths

The preceding analysis implies that emplacement of ultramafic material and overthrusting of a deepwater continental margin are not the primary sources of the subsurface loads acting on the Apennine, Carpathian and Hellenide forelands. The most obvious alternative is a deep source of loading related to plate subduction, either because of gravity acting on a very dense subducted plate (e.g., Malinverno and Ryan [1986] and Tomek et al. [1988]) or because of dynamic stresses related to subduction. To some extent it is difficult to separate these two

mechanisms, but the broad positive gravity anomalies present behind the Apennine, Carpathian and Hellenic thrust belts suggest that an anomalously dense mass is present in the approximate position where one would infer a subducted plate to be present. Along each profile (1-3), the observed Bouguer gravity anomalies over a zone at least several hundred kilometers wide are 50-100 mGal more positive than would be expected from simple isostatic compensation of the overriding plate (Figures 5-7 and 12-14).

19449194, 1993, 2, Downloaded from https://agupubs.onlinelibrary.wiley.com/doi/10.1029/92TC02248 by University Of British Columbia, Wiley Online Library on [23/07/2025]. See the Terms and Conditions

and-conditions) on Wiley Online Library for rules of use; OA articles are governed by the applicable Creative Commons License

Good fits between observed and computed gravity can be obtained by positioning a dense slab as shown in Figures 12-14. The geometry and total mass anomaly of the slab were constrained only by requiring a good fit to the observed gravity and by requiring a slab position that was geologically consistent with the known direction of subduction. The dense slabs inferred from this exercise extend from about 40 to 80 km depth and dip about 60° for the Carpathian system, extend from about 50 to 150 km depth and dip about 45° for the Apennine system, and extend from about 50 to 250 km depth and dip about 45° for the Hellenide system. Although deep and intermediate depth

19449194, 1993, 2, Downloaded from https://agupubs

onlinelibrary.wiley.com/doi/10.1029/92TC02248 by University Of British Columbia, Wiley Online Library on [23/07/2025]. See the Terms

onditions) on Wiley Online Library for rules of use; OA articles are governed by the applicable Creative Commons

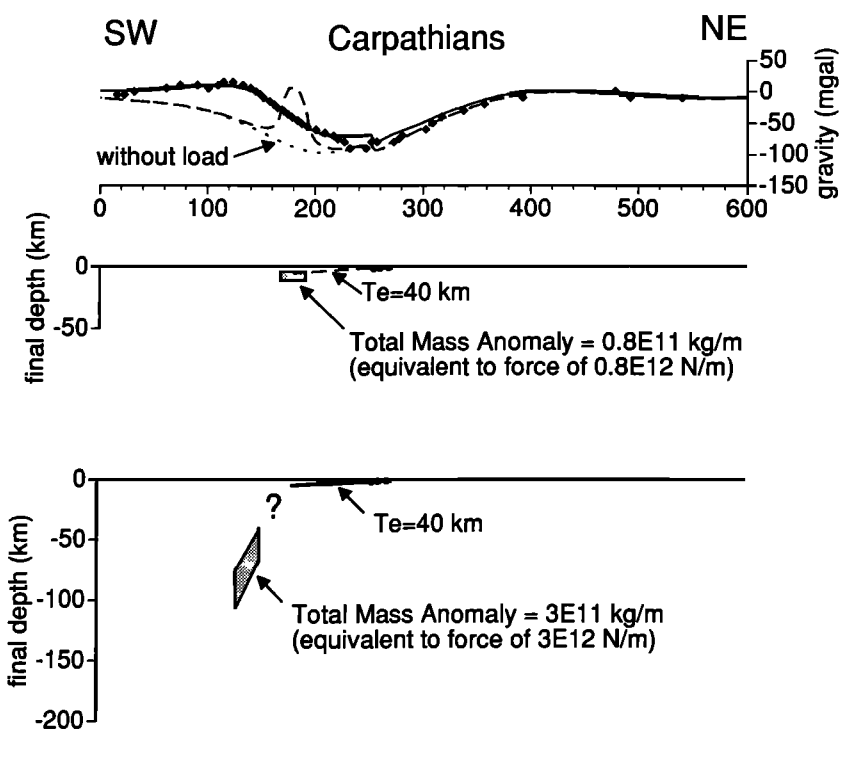


Fig. 13. (Top) Observed (symbols) and computed gravity anomalies across profile 2 (Carpathians) assuming that the subsurface load corresponds to a midcrustal mass anomaly (dashed line) or to a dense subducted slab at depth (solid line). Dotted line shows computed Bouguer anomalies corresponding to the best fitting deflection profile without accounting for the mass of the subsurface load. (Middle) Size and position of inferred midcrustal mass anomaly with a density contrast of 500 kg/m³. (Bottom) Inferred size and position of dense subducted slab dipping 60° and extending from 40 to 110 km depth.

earthquakes do not occur beneath profiles 1 and 2 (Apennines and Carpathians), the disappearance of several hundred kilometers of lithosphere beneath each thrust belt in Miocene-Quaternary time, the active Benioff zones present along strike from the inferred slab positions, and, in Italy, the results of seismic tomography, all suggest that a west or southwest dipping subducted slab at least several hundred kilometers in length should be present beneath these orogenic belts. Beneath profile 3 (Hellenides) a well-developed Benioff zone is present to 150 km depth, and the results of seismic tomography suggest that the slab may reach at least 450 km depth.

Is this long wavelength gravity anomaly over the inferred slab positions of a reasonable size to have been generated by the positive density contrast between subducted lithosphere and surrounding asthenosphere? Assuming an approximate density contrast of 100 kg/m³, this implies slabs with a cross-sectional areas of about 3000 km² (Carpathians), 5000 km² (Apennines) and 12,000 km² (Hellenides), which seems reasonable for slabs that may be perhaps several hundred kilometers in length (Figures 12-14). Even if the density contrast were smaller by a factor of 2 to 4, the cross-sectional areas would still be within a reasonable range.

A second observation that argues for the importance of negative slab buoyancy in driving subduction at retreating plate boundaries is the relationship between the density of the foreland lithosphere and the presence or absence of active subduction. Because there is an inverse relationship between

topographic elevation of the foreland and the average density of the underlying lithosphere, the topographic elevation (or bathymetry) of the foreland immediately in front of the subduction system is a direct measure of the density of the lithosphere entering the subduction zone; a deepwater environment indicates high-density lithosphere while a shallow water to nonmarine environment indicates a low-density lithosphere. In retreating subduction systems there is a good correlation between the cessation of subduction and the entry into the subduction system of foreland lithosphere with shallow water to nonmarine conditions. This indicates that the density of the subducted lithosphere is closely related to the subduction process and that subduction of low-density lithosphere cannot be sustained within retreating subduction systems.

Dynamic Stresses

It is likely that dynamic factors also affect the subducted slab. For example, the broad positive gravity anomalies present on profiles through the Apennines, Carpathians and Hellenides suggests a positive mass anomaly at depth that is approximately 2 to 4 times larger than that needed to explain the observed deflection of the foreland lithosphere in front of and beneath the thrust belts (Table 2 and Figures 12-14). This suggests that the dense slab at depth is partially supported by dynamic stresses within the asthenosphere, for example by viscous stresses acting to support the slab at depth. Thus dynamic stresses

Fig. 14. (Top) Observed (symbols) and computed gravity anomalies across profile 3 (southern Hellenides) assuming that the subsurface load corresponds to a midcrustal mass anomaly (dashed line) or to a dense subducted slab at depth (solid line). Dotted line shows computed Bouguer anomalies corresponding to the best fitting deflection profile without accounting for the mass of the subsurface load. (Middle) Size and position of inferred midcrustal mass anomaly with a density contrast of 500 kg/m³. (Bottom) Inferred size and position of dense subducted slab dipping 45° and extending from 50 to 270 km depth.

appear to retard, rather than facilitate, the sinking of the subducted lithosphere.

It is not possible to rule out completely the role of dynamic processes in driving upper plate extension and in creating the broad positive gravity anomalies observed behind the thrust belts in retreating subduction systems, but several observations suggest that this is not the dominant process. First, a longwavelength positive anomaly of +50 mGal is observed behind the Carpathian system where neither subduction nor extension has been active since about 10-12 Ma (Figure 13). Thus one would infer that any dynamic processes active during subduction and extension should have disappeared over this time interval. Second, the areal distribution of the longwavelength anomaly does not always coincide with the area of back arc extension and does not correlate with water depth. This is clearly illustrated in profile 2 through the Carpathians, where the positive gravity anomaly is perhaps 200 km in width but the extensional basin system is more than 500 km in width (Figure 13). On profile 3 through the southern Hellenides and the Aegean Sea the positive gravity anomaly occurs primarily east of the area of active extension. Thus the regional positive gravity anomalies on profiles 2 and 3 do not appear to be spatially correlated with extension. Third, the magnitude of the

long-wavelength gravity anomaly, +50 mGal behind the Apennines and Carpathians and +100 mGal over the Aegean Sea, implies about 700-1500 m of dynamically supported topography, which is roughly 3 to 5 times larger than the largest dynamically supported topography observed over mid-ocean swells (M. McNutt, personal communication, 1992). The magnitude of the gravity anomaly thus appears to be too large to be primarily due to dynamically compensated topography within the back are region.

19449194, 1993, 2, Downloaded from https://agupubs. onlinelibrary.wiley.com/doi/10.102992TC02248 by University Of British Columbia, Wiley Online Library on [2307/2025]. See the Terms and Conditions (https://onlinelibrary.wiley.com/terms-and-conditions) on Wiley Online Library for rules of use; OA articles are governed by the applicable Creative Commons. License

Summary

Taking all of these points together, it appears that the presence or absence of active subduction at retreating subduction boundaries can be correlated temporally and spatially with the density of the downgoing lithosphere. The broad positive gravity anomalies observed behind the thrust belts are probably not due to dynamic support of surface topography and can plausibly be considered to reflect a negatively buoyant subducted slab. Dynamic stresses acting on the downgoing plate appear to retard, rather than facilitate, subduction. Thus both subduction and upper plate extension at retreating plate boundaries appear to be driven primarily by the

19449194, 1993, 2, Downloaded from https://agupubs. onlinelibrary.wiley.com/doi/10.102992TC02248 by University Of British Columbia, Wiley Online Library on [2307/2025]. See the Terms and Conditions (https://onlinelibrary.wiley.com/terms-and-conditions) on Wiley Online Library for rules of use; OA articles are governed by the applicable Creative Commons. License

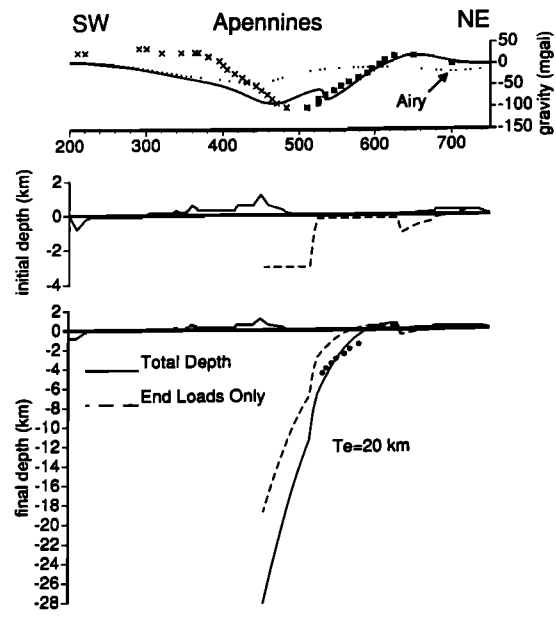


Fig. 15. Observed and computed flexure for profile 1 (Apennines) when initial water depth is forced to 3 km beneath the Apennines. (Top) Symbols show observed Bouguer gravity anomalies; solid symbols are observations used explicitly in computing the best fitting flexural profile. Solid line shows computed Bouguer anomalies corresponding to best fitting deflection profile for a water depth of 3 km beneath the Apennines. Dotted line shows Bouguer anomalies that would be expected if topography were Airy compensated. (Middle) Dashed line shows initial (preflexural) topography or bathymetry corresponding to the best fitting flexural profile. Solid line shows present-day topography. (Bottom) Symbols show observed depth of the foredeep basin. Solid curve shows best fitting flexural profile. Dashed curve shows component of flexural profile due to subsurface (subduction) loads.

negative buoyancy of the downgoing lithosphere, and these driving forces also manifest themselves in the flexural deflection of the foreland lithosphere and in the gravity signature behind the thrust belt. (An alternative view has been presented by Doglioni, 1992, who attributes the differences in tectonic style to the vergence of subduction with regard to eastward flow within the underlying mantle. However, because two of the three retreating plate boundary systems described here are westvergent and one is east vergent, the correlation between plate boundary style and mantle flow seems far from obvious.)

TOPOGRAPHIC VERSUS SUBDUCTION LOADING: WHY?

The relative importance of topographic loading at advancing subduction boundaries and subduction loading at retreating plate boundaries can perhaps be best understood in light of the extent to which thrust sheets are transported over the foreland (relative to the position at which subduction forces are applied to the plate). In particular, one might suspect that at advancing plate boundaries thrust sheets may be transported for great distances over the foreland because of the relatively large horizontal

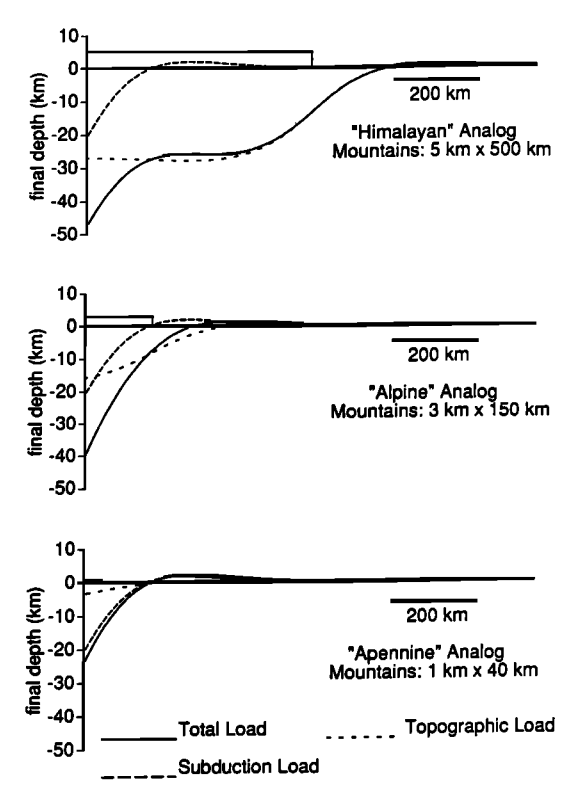


Fig. 16. Schematic diagram showing the interaction between topographic and subduction loads for the Himalayan, Alpine and Apennine systems. Effective elastic plate thickness is 30 km in each case. The terminal vertical shear force applied to each plate end is -4×10¹² N/m and the terminal bending moment is 2×10¹⁷ N. The topographic load corresponds to mountains 5 km high by 500 km wide (Himalayas), 3 km high by 150 km wide (Alps), and 1 km high by 40 km wide (Apennines). The deflections due to the topographic loads and the end loads (subduction loads) can be summed to give the total deflection, as shown.

compressional stresses that must act across the subduction boundary (they must be sufficiently large to produce horizontal shortening in the upper plate). In contrast, one might suspect that at retreating plate boundaries thrust sheets may be transported for only small distances over the foreland because of the relatively small horizontal compressional stresses that must act across the subduction boundary (they must be sufficiently small to allow horizontal extension in the upper plate).

Figure 16 shows the way in which the magnitude of thrust sheet transport (as well as the topographic elevation of the mountain belt) can affect the way in which flexure of the foreland lithosphere is compensated by topographic and subduction loads. Each profile in Figure 16 corresponds to a subducted and overthrust foreland lithosphere with the same flexural strength and subjected to the same subduction loads applied at the effective plate end. Profile 16A shows a situation analogous to an advancing plate boundary (the Himalayas) where the large horizontal compressional stresses acting across a plate boundary have created high topographic mountains and have transported the thrust belt for a great distance over the

foreland. Profile 16C shows a situation analogous to a retreating plate boundary (the Apennines), where the small horizontal compressional stresses acting across the plate boundary have created only low topographic mountains and have transported the thrust belt for a only a short distance over the foreland [see Lillie, 1991].

Flexural analysis of these two profiles would reveal that at the advancing plate boundary the foredeep basin subsidence is compensated almost completely by the topographic load represented by the mountain belt (although subduction load may be responsible for deflection of the subducted plate near the plate end). The same analysis at the retreating plate boundary would reveal that the foredeep basin subsidence is compensated almost completely by the subduction load acting on the subducted plate. This simplistic analysis indicates that differences in the magnitude of thrust sheet transport and in topographic elevation can directly control the relative importance of topographic and subduction loads in causing the flexural subsidence of the foreland lithosphere. (This example also implies that a significant subduction load might be present beneath southern Tibet and north of the Himalaya but, if a subduction load exists, it must be applied at a point sufficiently far from the foredeep basin that it does not affect the flexure of the lithosphere beneath the basin.)

A situation intermediate between these two end-member examples is illustrated in profile 16B (analogous to the Alps). In this example, the frontal thrusts are inferred to have advanced reasonably far over the foreland relative to the subduction system, but not so far as in profile A. The topographic elevation of the thrust belt is also high, but not so high as in profile A. Along profile B the foredeep basin is close enough to the effective plate end for the subduction load to have some effect on the deflection of the lithosphere beneath the basin. However, the deflection beneath the basin due to the subduction load is upward because the foreland basin coincides with the position of the flexural bulge generated by the subduction load. The total deflection beneath the foredeep basin, produced by summing the effects of the topographic and subduction loads, is less than one would expect from the topographic elevation of the mountains, while the deflection beneath the inner parts of the thrust belt are greater than one would expect from the topographic elevation of the mountains. This is similar to what is observed in the Alps and suggests that they represent an intermediate case between the extreme examples offered by the Apennine and Himalayan systems.

THE TECTONIC EXPRESSION OF SUBDUCTION AND CONVERGENCE RATE

The systematic differences in structure, metamorphism, sedimentation and deformation history at advancing and retreating subduction boundaries strongly suggests that these features, as well as the geometry of the adjacent foredeep basins, are genetically related to the forces that drive subduction and convergence. This section attempts to relate the development of each of these geological features to these fundamental driving forces. In particular, these geological features can be simply related to differences in the magnitude of horizontal compressional stresses and strains that are present at advancing and retreating subduction boundaries, and to the resulting differences in topographic elevation and crustal thickness.

Horizontal Compressional Stresses

Relatively large horizontal compressional stresses must act across advancing subduction boundaries because these stresses must be sufficiently large to produce regional horizontal shortening and thickening of continental crust within the upper plate. In contrast, relatively small horizontal compressional stresses must act across retreating subduction boundaries because these stresses must be sufficiently small to allow regional horizontal extension and thinning of continental crust within the upper plate. This conclusion is consistent with the state of stress inferred at advancing and retreating subduction boundaries from seismic studies of oceanic subduction zones [Uyeda and Kanamori, 1979; Ruff and Kanamori; 1980].

Topography, Back Arc Extension and Back Arc (Antithetic) Thrusting

Regional crustal shortening must occur at advancing subduction systems because, by definition, the distance between the trench (or foredeep basin) and the interior part of the overriding plate decreases with time. Thus the presence of topographically high mountains and the development of antithetic thrust belts above advancing subduction boundaries can be simply understood as the result of crustal shortening and thickening within the upper (and lower) plates. In contrast, all retreating subduction boundaries exhibit, by definition, a zone of crustal extension within the back are region because the distance between the trench (or foredeep basin) and the interior part of the overriding plate increases with time. The topographically low mountains present above retreating subduction boundaries also reflect the lack of crustal shortening on a regional scale within the overriding plate.

Erosion (or Denudation)

Differences in erosion (or denudation) rate at advancing and retreating subduction boundaries can be directly attributed to the presence or absence of topographically high mountains. Thus thrust belts developed above advancing plate boundaries with large topographic elevations and steep topographic slopes exhibit large amounts of erosion and denudation, while at retreating plate boundaries thrust belts with small topographic elevations and gentle topographic slopes exhibit small amounts of erosion.

Metamorphism

The metamorphic grade present in rocks exposed at the surface in the two tectonic settings is probably controlled to a large extent by differences in denudation rate and in the total denudation that has occurred within the two types of thrust belts. Most obviously, the large amount of denudation that occurs above advancing subduction boundaries commonly unroofs rocks to midcrustal levels, thus bringing to the surface rocks that have experienced high pressures and temperatures. This does not occur above retreating subduction boundaries. Less obviously, the rate of surface denudation within an orogenic system strongly controls the temperatures that prevail at a particular depth within the crust [Royden, 1992a]. Rapid denudation rates result in greatly elevated temperatures

throughout the crust, particularly if significant heat production is present within the crust. Thus the temperature at a given crustal depth will be greater above advancing subduction boundaries, where rapid denudation is common, than above retreating subduction boundaries, where little to no denudation usually occurs at the surface.

Deformation of Crystalline Basement

Two major factors appear to be responsible for the extent of crystalline basement deformation within thrust belts formed at advancing and retreating subduction boundaries. First, at advancing plate boundaries, horizontal compressional stresses large enough to result in shortening of the upper plate are transmitted across the subduction system, while at retreating plate boundaries the horizontal compressional stresses are sufficiently small to allow regional extension of the overriding plate. This also indicates that crystalline rocks of the downgoing plate must be subjected to much greater horizontal compressional stresses at advancing subduction boundaries than at retreating subduction boundaries. The presence or absence of penetrative shortening within crystalline rocks of the lower plate can thus be directly linked to the different magnitudes of horizontal compressional stress present in the two different types of subduction system. Second, the differences in denudation rate above advancing and retreating plate boundaries implies that, at a given crustal depth, temperatures within the crust are higher at advancing plate boundaries than at retreating plate boundaries, thereby facilitating deformation of crystalline basement at advancing plate boundaries due to weakening of the rocks with increasing temperature.

Postcollisional Convergence

The systematic differences in the postcollisional behavior of advancing and retreating subduction boundaries can be directly attributed to the forces that drive subduction and convergence across the plate boundary. Retreating subduction systems experience little postcollisional convergence and are only active in precollisional to syncollisional settings (see examples of Apennines, Carpathians and Hellenides described in Table 1 and Appendix B on microfiche). This behavior is evidence that the density of the downgoing plate is crucial in driving subduction at retreating plate boundaries and indicates that, when the buoyancy of the downgoing plate increases sufficiently, subduction stops. In contrast, advancing subduction systems may remain active for tens of millions of years after collision occurs, with overthrusting and apparent subduction of hundreds of kilometers of continental lithosphere (see examples of Alps and Himalayas described in Table 1 and Appendix B). This illustrates that a significant portion of the forces that drive convergence across these advancing plate boundaries is independent of the buoyancy of the subducted plate and must be due to far-field plate stresses related to the global motions of the large plates.

Foredeep Basin Geometry and Compensation

At advancing plate boundaries, topographic loads control much or all of the shape of the foredeep basin and subduction loads play little or no role in the downbending of the foreland. The foredeep basins thus developed are of approximately the depth that one would expect from the size of the adjacent mountain belts and flexural strength of the foreland lithosphere. In some cases, such as in the Alps, the foreland basin may actually be somewhat shallower than one would expect from the size of the adjacent mountains. At retreating plate boundaries the downward force of gravity acting on dense subducted lithosphere appears to be responsible for most of the downbending of the foreland lithosphere and, together with the flexural strength of the foreland lithosphere, controls much or all of the shape of the foredeep basin. The foredeep basins thus developed are generally much narrower and deeper than one would expect from the size of the adjacent mountain belts. This phenomenon can be simply explained by the mechanical coupling and horizontal stress transmission across the subduction boundary, resulting in very great transport of thrust sheets over the foreland at advancing plate boundaries and very little transport of thrust sheets over the foreland at retreating plate boundaries, as has been described in the preceding section.

Foredeep Basin Facies

In a complex interplay of tectonic processes, the forces that control convergence and subduction also affect the sedimentary facies deposited in the foreland basin adjacent to the orogenic belt. Retreating subduction boundaries are commonly active in a precollisional to syncollisional setting, involve subduction of a deepwater foreland throughout much of their history, and develop topographically low mountains and relatively deep foredeep basins. Such settings are conducive to the deposition of flysch (deepwater submarine fan deposits) within the foredeep basin, perhaps terminating with a short period of molasse deposition at the time of continental collision. Advancing subduction boundaries may be active in precollisional (e.g. the Andes) or postcollisional (e.g. the Alps and the Himalayas) settings, but are perhaps more common in postcollisional settings. After collision they commonly undergo a protracted history of postcollisional shortening and convergence, involving subduction (or at least overthrusting) of a shallow-water to nonmarine foreland and develop topographically high mountains and relatively shallow foredeep basins. Such settings are conducive to the deposition of molasse (shallow to nonmarine coarse clastic material) because the topographically high mountains commonly undergo rapid erosion, have steep topographic slopes that enable transport of very coarse material to the basin, and have a sediment supply sufficient to keep the foredeep basin filled over an extended period of time. In this way the protracted history of flysch deposition commonly observed at retreating subduction boundaries can be causally linked to the plate boundary setting within which subduction has occurred, while the protracted history of molasse deposition commonly observed at advancing subduction boundaries can likewise be linked to the plate boundary setting. In a sense the difference between foredeep basin facies is not controlled directly by plate boundary processes, but rather by the precollisional or postcollisional nature of the convergence. However, because only advancing subduction systems undergo significant postcollisional convergence, the facies are in large part indirectly controlled by the plate boundary processes.

DISCUSSION AND CONCLUSIONS

The five orogenic belts examined in this paper fall into two distinct categories, those in which subduction is contemporaneous with regional crustal extension in the overriding plate (Apennines, Carpathians, and Hellenides) and those in which subduction is contemporaneous with regional crustal shortening within the overriding plate (Alps and Himalayas). Within the framework of plate boundary processes, the former have developed at convergent boundaries where the rate of subduction exceeded the rate of overall plate convergence, termed here retreating plate boundaries, while the latter have developed at convergent boundaries where the rate of overall plate convergence exceeded the rate of subduction, termed here advancing plate boundaries. Within each category the orogenic systems examined in this paper display gross similarities in their structure, morphology, metamorphic and sedimentary facies, and deformation history (Table 2). This paper has attempted describe the systematic differences in the tectonic styles developed at advancing and retreating convergent boundaries, and to demonstrate that they are not coincidental but are rather an expression of the forces that drive subduction and plate convergence in these two fundamentally different plate boundary settings.

The dominant force that drives subduction at retreating subduction boundaries appears to be the negative buoyancy of the subducted plate, possibly enhanced by dynamic processes within the asthenosphere (although this study suggests that dynamic stresses acting on the downgoing plate retard, rather than facilitate, subduction). Regional extension within the overriding plate (e.g. back arc extension) behind these orogenic belts thus appears to be a passive phenomenon driven by the poor transmission of horizontal compressional stress across the adjacent subduction boundary. Across advancing subduction boundaries, convergence appears to be mainly driven by farfield stresses that govern the global plate motions of the large plates. (This does not preclude the possibility that negative buoyancy of the subducted plate, or other subduction forces, are of great importance in driving convergence in regions where the subducted plate has a high density, such as along the northern and western margins of the Pacific plate.) These fundamental driving forces are clearly expressed in the regional deformation of the overriding plate at the subduction boundary (extensional at retreating subduction boundaries and compressional at advancing subduction boundaries) and in the importance of the subduction load in controlling the flexural bending of the foreland lithosphere in front of the orogenic belt.

The concept that orogenic belts formed above advancing subduction boundaries have different and recognizable tectonic signatures from those formed above retreating subduction boundaries can perhaps help one to better understand the plate boundary settings in which ancient orogenic belts have been formed. This study suggests that both ancient and modern continental subduction zones and orogenic belts can be divided into segments that have formed at advancing plate boundaries and segments that have formed at retreating plate boundaries, and that the different settings can be recognized by the tectonic style of the orogenic belt. Orogenic belts that form at advancing subduction boundaries are commonly typified by topographically high mountains, the development of antithetic thrust belts, rapid rates of erosion and denudation, exposure of

high-grade metamorphic rocks at the surface, extensive involvement of crystalline basement in shortening, large amounts of postcollisional convergence, and during postcollisional convergence by a protracted history of molasse deposition within the adjacent foredeep basin(s). Orogenic belts that form at retreating subduction boundaries are commonly typified by topographically low mountains, the development of "back arc" extensional basins, little to no erosion or denudation, low-grade to no metamorphism, little involvement of crystalline basement in thrusting, little to no postcollisional convergence, and by a protracted history of flysch deposition within the adjacent foredeep basin.

These thrust belt characteristics are only those that are commonly, but not always, associated with the two different types of plate boundary setting. One or more of these characteristics may be absent within a particular convergent belt, particularly when the belt is observed a short time after a change in its plate boundary setting and the characteristic features have not had sufficient time to develop. In general, however, most thrust belts formed at convergent zones within the continental lithosphere can probably be readily identified as having formed at advancing or retreating subduction boundaries by the systematic expression of morphologic and structural style, metamorphic grade, and foredeep basin geometry and facies. Because subduction boundaries may evolve from advancing to retreating boundaries, or vice versa, one must be sure that the features of the orogenic system that one wishes to categorize are contemporaneous with one another.

There are probably a number of different ways in which plate boundaries evolve from one type to another. For example, orogenic belts that have formed above subduction boundaries at which the subduction and convergence rates are nearly equal may alternate back and forth between the two different tectonic styles without apparent cause. Retreating subduction boundaries appear to be especially common features in the early stages of collision along irregularly shaped continental boundaries, where they develop by subduction of dense lithosphere contained in oceanic embayments in the converging continents (for a discussion of this process in the Mediterranean region see Royden and Burchfiel [1989] and Royden [1992b]). Subduction boundaries may also evolve from advancing to retreating boundaries, or vice versa because of changes in local convergence rates or large scale changes in global plate motions. The process of continuing continental collision also appears to facilitate changes in plate boundary style. For example, in the retreating subduction systems examined in this paper, subduction forces were clearly diminished during continental collision as the buoyancy of the subducted plate increased, so that the time of continental collision is a likely point at which a retreating subduction boundary may be transformed into an advancing subduction boundary (if subduction does not cease altogether).

The discussion in this paper only pertains to subduction boundaries located entirely within continental lithosphere, but it seems probable that similar differences in tectonic style can be observed at subduction boundaries where oceanic lithosphere is subducted beneath continental lithosphere. A good example of such an orogenic belt developed above an advancing plate boundary is the South American Andes, which displays high topography, an antithetic thrust belt and a topographically compensated, molasse-filled foredeep basin on its east side

19449194, 1993, 2, Downloaded from https://agupubs.onlinelibrary.wiley.com/doi/10.1029/92TC02248 by University Of British Columbia, Wiley Online Library on [23.07/2025]. See the Terms and Conditions (https://onlinelibrary.wiley.com/terms-and-conditions) on Wiley Online Library for rules of use; OA articles are governed by the applicable Creative Commons License

[Lyon-Caen et al., 1985]. (Some of the characteristic features of advancing plate boundaries are missing in the Andes, particularly a deep level of erosion and the exposure of highgrade rocks at the surface. This is probably due to the dry climate west of the Andes and the youth of the topographic mountains.) Examples of orogenic belts developed above retreating plate boundaries where oceanic lithosphere is subducted are reasonably common, for example the Okinawa Trough above the subducting Pacific plate is a site of active back arc extension within the continental lithosphere and displays most of the morphological and structural features associated with retreating orogenic belts [Kimura et al., 1986; Nagumo et al., 1986]. Within the geologic record, the alternation in tectonic style developed along the western margin of North America, which has been an active subduction boundary since late Paleozoic time, suggests an alternation between advancing and retreating plate boundary systems during a protracted history of oceanic subduction along this margin.

APPENDIX A: POTENTIAL SOURCES OF ERROR IN COMPUTING SUBSURFACE LOADS

The accuracy with which the relative roles of subsurface and topographic loads can be computed are perhaps best illustrated by example. Figure A1 illustrates the sensitivity of the results to the flexural strength assumed for the foreland lithosphere. The best results for flexure of the Adriatic lithosphere in Profile 1 were obtained using an effective elastic plate thickness of 20 km. When the maximum and minimum allowable values of 10 and 30 km for the effective elastic plate thickness are used, the total deflection of the lithosphere is similar to that computed in the 20-km case, although the resulting profiles do not fit the deflection data very well beneath the foredeep basin. Nevertheless, the relative roles of the topographic and subsurface loads change very little from the case where the effective elastic plate thickness is 20 km, and the subsurface load dominates the deflection. Perhaps more importantly, the size of the subsurface load, as defined by the magnitude of the vertical shear force applied at the effective plate end, varies very little between the three cases (at $2.1 \times 10^{12} \pm 0.4 \times 10^{12}$ N/m. Table 3). Thus the computation of topographic and subsurface loading is not sensitive to the strength assumed for the foreland lithosphere, provided that a reasonable fit to the deflection and gravity data can be obtained.

The deflection due to subsurface loads is also not very sensitive to to assumptions about the initial water depth. In computing the results for profiles 1-6, the initial water depth is assumed to be uniform beneath the thrust belt and most of the foreland basin. However, if the water depth beneath the thrust belt increases markedly, then one may seriously underestimate the size of the topographic load. For example, along profile 1 through the Apennines the initial water depth is computed to be 630 m prior to loading. If this is increased by several kilometers beneath the thrust belt, the topographic load may have been severely underestimated. Figure 15 shows the best fit flexural solution that is obtained by fixing the initial water depth at 3 km beneath the thrust belt, but solving for the best fitting initial water depth elsewhere. The resulting fit to the gravity data is reasonable, although the fit to the depth data is poor. When the total deflection is broken down into topographic and subsurface components, the contribution of the

Fig. A1. Observed and computed flexure for profile 1 (Apennines) when effective elastic plate thicknesses are assumed to be 10 and 30 km. (Top) Symbols show observed Bouguer gravity anomalies; solid symbols are observations used explicitly in computing the best fitting flexural profile. Lines show computed Bouguer anomalies corresponding to the best fitting deflection profile for each plate strength. (Middle) Symbols show observed depth of the foredeep basin. Curve shows best fitting flexural profile for an effective elastic plate thickness of 10 km. Dashed curve shows component of flexural profile due to subsurface (subduction) loads. (Bottom) Symbols show observed depth of the foredeep basin. Curve shows best fitting flexural profile for an effective elastic plate thickness of 10 km. Dashed curve shows component of flexural profile due to subsurface (subduction) loads.

topographic load to the plate flexure can be seen to be much larger. However, the total deflection is also larger by a comparable amount and the deflection due to the subsurface load is mostly unchanged (the terminal force is reduced from -2.1×10¹² N/m to -2.0×10¹² N/m, or by about 5%, Table 3). Thus increasing the initial water depth beneath the thrust belt (relative to the initial water depth beneath the foredeep basin) can increase the deflection due to the topographic load but leaves the deflection due to the subsurface load mostly unchanged. Even in the extreme case shown in Figure 15, where the fit to the deflection data in the foreland becomes unacceptably poor, the subsurface load still contributes about two thirds of the total deflection at the plate end. (For a discussion of the effects of nonuniform water depths within the basin itself, see Royden [1988] for a similar conclusion.)

The examples in Figures A1 and 15 illustrate that computation of the subsurface load and its contribution to the deflection of the foreland lithosphere is quite robust. The reason for this can be seen by examining the relationship between the gravity signal across the orogenic system and the vertical shear force acting on the plate end. The difference

TABLE 3. Flexural Parameters and Loads Used on Profile 1 (Figures A1 and 15)²

	Figure A1	Figure A1	Figure 15
Effective elastic plate thickness (km)	10	30	20
Flexural rigidity (Nm)	7.2×10 ²¹	1.9×10 ²³	5.7×10 ²²
Position of effective plate end $(km)^b$	475	455	455
Vertical shear force at plate end (N/m) ^c	-2.5×10 ¹²	-1.8×10 ¹²	2.0×10 ¹²
Bending moment plate end (N/m) ^d	0.0×10 ¹⁷	1.9×10 ¹⁷	1.2×10 ¹⁷

a Densities and basin coordinates are the same as those given for profile 1 in Table 2.

between the observed Bouguer anomaly and the Bouguer anomaly that would be expected if all topography were Airy compensated (defined here as the isostatic anomaly) gives a measure of the extent to which the topography is not locally compensated. Integration of the isostatic anomaly across the orogenic system provides a measure of the departure of the mountains and the adjacent foredeep basin from apparent regional isostatic equilibrium. If the mountains and the adjacent basin are to be regionally compensated then they must be subjected to an additional force acting on the plate that does not show up in the gravity signal. By equating this additional force with the subsurface load, the size of the subsurface load can be inferred directly from observations of topography and gravity across the subduction system. This result is independent of the rheology assumed for the foreland and does not rely on the assumption of an elastic foreland lithosphere. Additional details about the subsurface load can, of course, be better constrained by combining gravity data with information about the plate deflection beneath the foredeep basin and in the foreland. (Note that the bending moment needed at the plate end to maintain the observed deflection is somewhat arbitrary because it can be easily changed by adding a short length of weak lithosphere onto the end of the subducted lithosphere. However, the values of vertical shear force needed at the plate end in order to maintain the observed deflections are quite robust, as is the approximate flexural geometry of deflection due to the subsurface loads.)

Another possible source of error is the neglect of possible horizontal compressional stresses in computing the flexure of

the subducted lithosphere. This is probably reasonable for the Apennine, Carpathian and Hellenic subduction systems where the upper plate is in regional extension, but for the Alps and Himalayas it may be that significant horizontal compressional stresses act on the flexing lithosphere. However, it is not clear what the magnitude of such stresses should be, and the error induced by adding such a correction could be larger than the correction itself. In addition, the effect of horizontal compressive stresses appears primarily in the estimated elastic thickness of the plate, not in the shape it assumes (e.g. Judge and McNutt [1991]). Thus in neglecting horizontal compression, it is possible that the values of flexural rigidity computed have been underestimated, but computation of the deflection profile and the vertical shear force acting at the plate end should not be significantly affected.

Acknowledgments. Special thanks are due to Clark Burchfiel for help and encouragement.

This research was supported by NASA grant NAG-532 and by a NSF Presidential Young Investigator Award to Leigh Royden. Portions of the paper on the Ionian Sea region were funded by NASA grant NAGW-1951. The manuscript was completed while Leigh Royden was on sabbatical at Caltech, supported by the Visiting Professorships for Women Program at NSF and by the Division of Geological and Planetary Sciences at Caltech. Printed copies (instead of microfiche) of Appendix B, "Geological and Tectonic Summaries of Five Orogenic Belts", can be obtained from the author upon request.

REFERENCES

Beck-Mannagetta, P., and A. Matura, Geological Map of Austria, 1:1,500,000, in Outline of the Geology of Austria and Selected Excursions, edited by G. Bundesanstalt, pp. 100-101, F. Berger and Soehne OHG, Hom, Vienna, Austria, 1980.

Bureau Gravimetrique International (en collaboration avec les Services Nationaux Interesses), Cartes mondiales de anomalies de Bouguer, scale 1:1,000,000 (Vienna Sheet), Paris, France, 1962-63.

Bureau Gravimetrique International (en collaboration avec les Services Nationaux Interesses), Cartes mondiales de anomalies de Bouguer, scale 1:1,000,000 (Budapest Sheet), Paris, France, 1964-65.

Cooper, J.C., The geology of the central Apennines

and foreland basin, Italy, Ph.D. thesis, Rice University, Houston, Texas, 1988.

Cross, T.A., and R.H. Pilger, Controls of subduction geometry, location of magmatic arcs, and tectonics of arc and back-arc regions, Geol. Soc. Am. Bull., 93, 545-562, 1982.

Doglioni, C., Main differences between thrust belts, Terra Nova, 4, 152-164, 1992.

b Relative to coordinates shown in Figures A1 and 15.

Negative values are downward force.

d Positive values correspond to concave downward curvature.

- Fuchs, W., Die Molasse und ihr nichthelvetischer Vorlandanteil am Untergrund einscliesslich der Sedimente auf der Boehmischen Masse, in Der Geologische Aufbau Oesterreichs, edited by R. Oberhauser, 144-176, Springer-Verlag, New York 1980.
- Gansser, A., The Geology of the Himalaya, 289 pp., Wiley Interscience, New York, 1964.
- Intergovernmental Oceanographic Commission, International bathymetry chart of the Mediterranean with Bouguer gravity anomalies, scale 1:1,000,000, Head Department of Navigation and Oceanography of the USSR, Ministry of Defense, Leningrad, USSR, 1989.
- Jarrard, R.D., Causes of compression and extension behind trenches, *Tectonophysics*, 132, 89-102, 1986a.
- Jarrard, R.D., Relations among subduction parameters, Rev. Geophys., 24, 217-284, 1986b.
- Judge, A., and M. McNutt, The relationship between plate curvature and elastic plate thickness: A study of the Peru-Chile trench, J. Geophys. Res., 96, 16,625-16,639, 1991.
- Karner, G.D., and A.B. Watts, Gravity anomalies and flexure of the lithosphere at mountain ranges, Jour. Geophys. Res, 88, (B12), 10,449-10,477, 1082
- Karunakaran, C. and R.R. Rao, Status of exploration for hydrocarbons in the Himalayan region: Contributions to stratigraphy and structure, Proceedings of the Himalayan Geology Seminar, New Delhi, India, Sept. 13-17, 1976, 1-72, 1976.
- Kimura, M., I. Kaneoka, Y. Kato, S. Yamamoto, I. Kushiro, H. Tokuyama, H. Kinoshita, N. Isezaki, N. Masaki, A. Oshida, S. Uyeda, and T.W.C. Hilde, Report on DELP 1984 cruises in the middle Okinawa Trough, part V, Topography and geology of the central grabens and their vicinity, Bull. Earthquake Res. Inst., 61, Univ. Tokyo, 269-310, 1986.
- Kollmann, K., and O. Malzer, Die Molassezone Oberoesterreichs und Salzburgs, in *Erdoel und Erdgas in Oesterrreich*, edited by F. Brix and O. Schultz, pp. 179-201, Naturhistorisches Museum Wien und F. Berger, Horn, Austria, 1980.
- Kruse, S.E., Deformation of continental lithosphere: Studies in the Ural Mountains, the Adriatic region, and the western United States, Ph.D. thesis, Mass. Inst. Technol., Cambridge, Massachusetts, 1989.
- Lillie, R.J., Evolution of gravity anomalies across collisional mountain belts: Clues to the amount of continental convergence and underthrusting, *Tectonics*, 10, 672-687, 1991.
- Lyon-Caen, H., and P. Molnar, Constraints on the structure of the Himalaya from an analysis of gravity anomalies and a flexureal model of the lithosphere, J. Geophys. Res., 88, 1251-1254, 1983.

- Lyon-Caen, H., and P. Molnar, Gravity anomalies, flexure of the Indian plate, and the structure, support, and evolution of Himalaya and Ganga Basin, Tectonics, 4, 513-538, 1985.
- Lyon-Caen, H., and P. Molnar, Constraints on the deep structure and dynamic processes beneath the Alps and adjacent regions from an analysis of gravity anomalies, Geophys. J. Int., 29, 19-32, 1989
- Lyon-Caen, H.M., P. Molnar, and G. Suarez, Gravity anomalies and flexure of the Brazilian shield beneath the Bolivian Andes, Earth. Planet. Sci. Lett., 75, 81-92, 1985.
- Malinverno, A., and W.B.F. Ryan, Extension of the Tyrrhenian Sea and shortening in the Apennines as result of arc migration driven by sinking lithosphere, *Tectonics*, 5, 227-245, 1986.
- Molnar, P., and T. Atwater, Inter-arc spreading and Cordilleran tectonics as alternates related to the age of the subducted lithosphere, Earth Planet. Sci. Lett., 41, 330-340, 1978.
- Molnar, P., and Q. Deng, Faulting associated with large earthquakes and the average rate of deformation in cental and eastern Asia, J. Geophys. Res., 89, 6203-6228, 1984.
- Morelli, C., et al., Regional geophysical study of the Adriatic Sea, Boll. Geofis. Teor. Appl., 11, 3-56, 1969.
- Morelli, C., G. Gantar and M. Pisani, Bathymetry, gravity and magmatism in the strait of Sicily and the Ionian Sea, Boll. Geofis. Teor. Appl., 11, 3-190, 1975.
- Moretti, I., and L. Royden, Deflection, gravity anomalies and tectonics of doubly subducted continental lithosphere: Adriatic and Ionian Seas, Tectonics, 7, 875-893, 1988.
- Nagumo, S., H. Kinoshita, J. Kasahara, T. Ouchi, H. Tokuyama, S. Asanuma, S. Koresawa and H. Akiyoshi, Report on DELP 1984 cruises in the middle of Okinawa Trough, part II, Seismic structural studies, Bull. Earthquake Res. Inst., 61, 167-202. 1986.
- Ogniben, L., M. Parotto, and A. Praturion, Structural Model of Italy, 502 pp., Consiglio Nazionale Delle Ricerche, Rome, 1975.
- Paraschiv, D., Romanian Oil and Gas Fields, 282 p., Institute of Geology and Geophysics, Bucharest, 1979.
- Pieri, M., and G. Groppi, Subsurface Geological Structure of the Po Plain, Italy, Final Geodyn. Proj. Publ. 414, 1-13, 1981.
- Royden, L., The steady-state thermal structure of eroding orogenic belts and accretionary prisms, J. Geophys. Res., in press, 1992a.
- Royden, L., The evolution of retreating subduction boundaries formed during continental collision, Tectonics, in press, 1992b.
- Royden, L., Late Cenozoic tectonics of the Pannonian

- bansin system, in *The Pannonian Basin: A Study* in *Basin Evolution*, edited by L. Royden and F. Horváth, Mem., *AAPG*, 27-48, 1988a.
- Royden, L., Flexural behavior of the continental lithosphere in Italy: Constraints imposed by gravity and deflection data, J. Geophys. Res., 93 (B7), 7,747-7,766, 1988b.
- Royden, L., and G.D. Karner, Flexure of the lithosphere beneath Apennine and Carpathian foredeep basins: Evidence for an insufficient topographic load, AAPG Bull., 68, 704-712, 1984.
- Royden, L., and B.C. Burchfiel, Are systematic variations in thrust belt style related to plate boundary processes? (The Western Alps versus the Carpathians), Tectonics, 8, 51-61, 1989.
- Roure, F., P. Heitzmann, and R. Polino, Deep structure of the Alps, Soc. Geol. Suisse Mem., vol. 1, 367 pp., Societe Geologique Suisse, Zürich, 1990.
- Ruff, L., and H. Kanamori, Seismicity and the subduction process, Phys. Earth Planet. Inter., 23, 240-252, 1980.
- Schweizerische Geophysikalische Kommission, Schwere-Karte der Schweiz, Bouguer-Anomalien, scale 1:500,000., 1979.
- Stockmal, G.S., and C. Beaumont, Geodynamic models of convergent margin tectonics: the southern Canadian Cortillers and the Swiss Alps, in Sedimentary Basins and Basin-Forming Mechanisms, edited by C. Beaumont and A.J. Tankard, Mem. Can. Soc. Petr. Geol., 12, 393-411, 1987.
- Tomek, C., L. Dvorakova, I. Ibrmajer, R. Jiricek and T. Korab, Crustal profiles of active continental collisional belt, Geophys. J. R. Astron. Soc., 89, 383-388, 1988.
- Trümpy, R., Geology of Switzerland, A Guidebook, Part A, An Outline of the Geology of the Geology of Switzerland, 104 pp., Wepf and Company, Basel, Switzerland, 1980.
- Uyeda, S., and H. Kanamori, Back-arc opening and the mode of subduction, J. Geophys. Res., 84, 1049-1061, 1979.
- Vurov V.C., I.B. Vishchijkov, V.V. Glushchko, G.D. Dosin, S.S. Kruglov, V.V. Kuzovenko, V.G Sviridenko, S.E. Smirhov, J.V. Sovchik, V.N. Utrodin, and V.A. Shenhakin, Tectonics of the Ukrainian Carpathians (in Russian), 152 pp., Ministry of the Ukrainian Socialist Republic, Kiev, 1986.
- L. H. Royden, Department of Earth, Atmospheric, and Planetary Sciences, Massachusetts Institute of Technology, Cambridge, MA 02139.

(Received March 25, 1992; revised September 8, 1992; accepted September 18, 1992.)